POLITECNICO
MILANO 1863

SCUOLA DI INGEGNERIA INDUSTRIALE
E DELL'INFORMAZIONE

Mechanical characterization of aerospace grade stainless steels produced by AM

TESI DI LAUREA MAGISTRALE IN
AERONAUTICAL ENGINEERING
INGEGNERIA AERONAUTICA- Indirizzo PROPULSIONE

Author: **Davide Maramonti**

Student ID: 952303
Advisor: Antonio Mattia Grande
Co-advisor: Tommaso Tirelli
Academic Year: 2022-2023

Abstract

In the last years the use of AM technologies has increased a lot, especially for Aerospace, Automotive, and medical sector [1].

This could be explained since these sectors are typically characterized by a higher complexity of their parts, and this means that a part can have a higher value. So the market allows a higher price that permits adoption of an expensive process, like AM.

The companies, universities and researchers are doing a great work to characterize and to establish regulations in order to guarantee a certain type of properties for each material, each technology and each machine.

A key topic is represented by raw materials for AM, which cost is very expensive even if in AM processes materials does not count more than 15-30 years.

Recent studies have shown also the environmental sustainability of AM since nowadays there is the possibility to use the recycled powder as feedstock for MBJ (Metal Binder Jetting) and LPBF (Laser Powder Bed Fusion).

In this thesis it is analyzed different configuration of different types of Steel (17-4 PH and 316L) produced with different technologies (MBJ and LPBF) from a static Point of view (tensile test) and from a dynamic one (fatigue test).

LPBF is a consolidated technologies with good properties but is not always appropriate for medium/ high production series of small parts.

On the other hands MBJ is appropriate to medium production of small parts but not many data are available in literature or from machine producers.

A total of 110 samples has been tested during this characterization studies

A lot of work must be done in order to guarantee the repeatability of the process of MBJ since is a new technology and not many studies have been carried out until now.

Keywords: MBJ, LPBF, fatigue, tensile test,17-4 PH, 316L

Abstract in italiano

Negli ultimi anni l'uso delle tecnologie Additive è cresciuto molto, specialmente nei settori *Aerospace*, *Automotive* e medicale.

Questo incremento è dovuto al fatto che questi settori sono solitamente caratterizzati da una grande complessità delle parti e ciò significa che ogni parte ha un grande valore (economico e tecnologico) e questo consente di avere un più alto valore di mercato, rendendo economicamente favorevole l'utilizzo di tecnologie costose, come l'AM.

Le aziende, le università e I ricercatori stanno facendo un grande lavoro per caratterizzare e fornire normative di riferimento per garantire delle specifiche proprietà per ogni materiale, prodotto con differenti tecnologie e macchinari.

Il vero problema per un maggior impiego di tali tecnologie è il costo proibitivo del materiale grezzo, oltre al costo di impianto delle macchine.

Recenti studi hanno dimostrato la sostenibilità ambientale del processo AM; infatti oggi è possibile usare polvere proveniente da materiali riciclati per il MBJ e il LPBF.

In questa tesi sono analizzate diverse configurazioni di differenti tipi di acciaio inossidabile (316L e 17-4 PH) prodotti con differenti tecnologie (MBJ e LPBF) da un punto di vista statico (prova di trazione) e da un punto di vista dinamico (test di fatica).

LPBF è una tecnologia consolidata con buone proprietà ma non è adatta a una produzione di serie medio/grande di piccole parti.

D'altra parte, il MBJ è stato realizzato per una media produzione di piccole parti, ma non ci sono molti dati disponibili nemmeno dalle aziende produttrici di macchinari.

Un totale di 110 provini sono stati testati durante questo studio di caratterizzazione.

Pertanto risulta necessario sostenere un grande lavoro per garantire ripetibilità del processo e per il MBJ dato che è una tecnologia nuova e alla quale non sono stati dedicati tanti studi.

Parole chiave: MBJ, LPBF, fatica, test di trazione, 17-4 PH, 316L

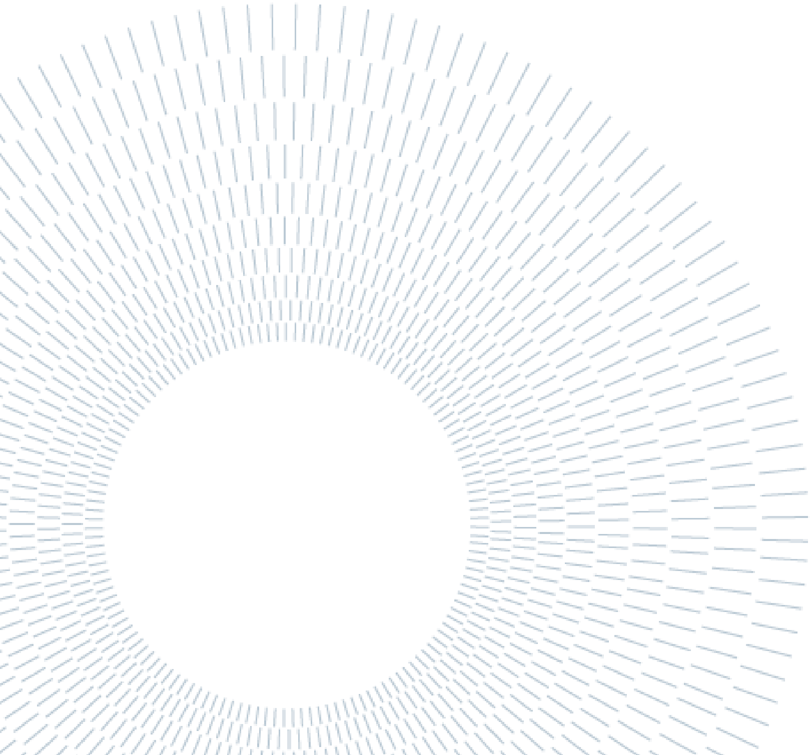

Contents

Abstract ..... **i**
Abstract in italiano ..... **iii**
Contents ..... **vii**
Glossary ..... **ix**
List of Figures ..... **xi**
Introduction **1**
1 General Characteristic of AM **7**
  1.1. Pre-processing file 8
  1.2. Orientation building 9
  1.3. Supporting 9
  1.4. Staircase effect 10
  1.5. Post-processing 10
2 PBF and MBJ **11**
  2.1. LPBF 13
  2.2. EBM 14
  2.3. MBJ 15
  2.4. MBJ vs LPBF process 17
3 Powder characterization **18**
  3.1. PSD 18
  3.2. Flowability 20
4 Mechanical characterization of materials **21**
  4.1. Tensile test 21
  4.2. Density measure 23
  4.3. Fatigue test 24
    4.3.1. Definition of fatigue cycles 26
    4.3.2. Wohler diagram 27
    4.3.3. Statistical method for evaluating fatigue limit 27
    4.3.4. Staircase 29
  4.4. Specimen geometry and preparation 30

5 Chemical characterization of materials 31
5.1. 316L austenitic stainless steel 31
5.2. 17-4 PH martensitic stainless steel 32
6 Parameter definition 33
6.1. Aidro by Desktop Metal 33
6.2. Eos M290 33
7 Heat treatment 35
7.1. HIP 35
7.2. H900 36
8 Analysis of result 37
8.1. Mechanical properties 37
8.1.1. Tensile test 38
8.1.2. Fatigue test 47
8.2. Density measurements 55
8.3. Porosity 59
8.3.1. Stencils preparation 59
8.4. Fracture analysis 63
8.4.1. SEM 63
8.4.2. Fractography 64
9 Conclusion and future developments 68
9.1. Porosity 68
9.2. Tensile test 70
9.3. Fatigue test 70
9.4. Future developement 71
Bibliography 73
A Appendix A Tensile test 77
B Appendix B Fatigue test 81
C Appendix C Porosity measures 82
D Appendix D density measures 88
Ringraziamenti 89

Glossary

AB: As built

AM: Additive Manufacturing

ASTM American society for testing and materials

BSE Back scatter electron

CDF: cumulative density function

DM: Desktop Metal

EBM: electron beam melting

EDM: Electrical Discharging Machine

HIP: hot isostatic pressure

HT: heat treatment

LCA: Life cycle assessment

LMS: least mean squares

LPBF: laser powder bed fusion

MBJ: metal binder Jetting

MIM: Metal injection Molding

ML: maximum Likelihood

PBF: Powder bed fusion

PH: precipitation hardening

PSD: powder spectral density

SEM Scanning electron microscope

SLM: selective laser melting

List of Figures

Figure 1: Shop system by DM [1] 2
Figure 2: Curing oven and depowdering station [2] 2
Figure 3: Furnace [2] 3
Figure 4: X25 Pro [3] 3
Figure 5: EOS M290 [4] 4
Figure 6: HIP treatment 5
Figure 7: H900 thermal cycle 5
Figure 8: trend N part vs cost per part [5] 7
Figure 9: Oriented specimens[5] 9
Figure 10: different types of supports [6] 9
Figure 11: Staircase effect 10
Figure 12: pistons system [7] 11
Figure 13: Gas atomization on the left and water atomization on right [8] 13
Figure 14: pistons system [5] 14
Figure 15: Electron Beam melting [5] 15
Figure 16: Metal Binder Jetting [7] 15
Figure 17: Metal Binder Jetting process 17
Figure 18: Powder particle x250 and x 1500 19
Figure 19: PSD of 17-4 PH 19
Figure 20: equipment for flowability test [9] 20
Figure 21: Angle of repose 20
Figure 22: stress strain diagram 22
Figure 23: find Rp 02 23
Figure 24: different type of fatigue cycles 25
Figure 25: Alternate fatigue cycle 26
Figure 26: different cycles respect to R 26

Figure 27: typical fatigue curve 27
Figure 28: typical Stair case 29
Figure 29: Geometry of tensile specimen and fatigue specimen 30
Figure 30: Furnace retort 30
Figure 31: EOS steel plate 34
Figure 32: Steelplate after stress relief during EDM cut 34
Figure 33: HIP thermal cycle 35
Figure 34: H900 thermal cycle 36
Figure 35: Lab furnace 36
Figure 36: Tensile test and extensometer 39
Figure 37: Tensile test 316 L AB in X and Z direction 40
Figure 38: 316 L broken specimen 40
Figure 39: Tensile test 316 L HIP 41
Figure 40: broken specimen 42
Figure 41: Tensile test of 17-4 PH 42
Figure 42: broken 17-4 PH specimen 43
Figure 43: Tensile test in 17-4 PH HIP 43
Figure 44: Tensile test 17-4 PH H900 44
Figure 45: broken H900 specimen 45
Figure 46: 17-4 PH MBJ HIP+H900 45
Figure 47 :broken specimen 17-4 PH 46
Figure 48 Tensile test 17-4 PH LPBF 46
Figure 49: Tensile test 17-4 PH LPBF H900 47
Figure 50: Broken specimen of 17-4 PH H900 47
Figure 51: LMS fatigue approximation 50
Figure 52: ML fatigue approximation for MBJ H900 samples 51
Figure 53 confidence bound of 95% respect to 5% percentile 53
Figure 54: comparison between interpolated data ML vs LMS 53
Figure 55: Fatigue life of 17-4 PH H900 LPBF with LMS Method 55
Figure 56: Fatigue life and 5% percentile of 17-4 PH H900 LPBF 56
Figure 57: comparison between ML and LMS of 17-4 PH H900 LPBF 56

Figure 58: balance used in density measurements 57
Figure 59: density measurement for 17-4 PH 58
Figure 60: density measurement for 316L.. 58
Figure 61: Sampled Areas.. 59
Figure 62: sample orientation in microscope.. 60
Figure 63: Cutted cube 60
Figure 64: lapped cube 60
Figure 65: SEM HitachiTM3000... 61
Figure 66: example of sampled section 62
Figure 67: density from SEM imagins 63
Figure 68: broken specimen after tensile test 65
Figure 69: dimples and trans granular fracture 66
Figure 70: Intergranular fracture without dimples 67
Figure 71: comparison fatigue data between LPBF and MBJ of 17-4 PH 69
Figure 72: comparison density measure between each condition................................. 70
Figure 73: comparison fatigue data between LPBF and MBJ of 17-4 PH 71

Introduction

1.1 Purpose of this thesis

In this work it will be presented a mechanical characterization of two types of stainless steel printed in different material and different heat treatments.

These two types of steel are:

- 316L an austenitic stainless steel with good corrosion resistance and good mechanical properties
- 17-4 PH a martensitic stainless steel with lower corrosion resistance but higher mechanical properties

The thesis will be organized in a first part where there will be a presentation of Additive Manufacturing technologies (general building principle, advantage, disadvantage) and a focus on MBJ and LPBF, the two used in this work.

Subsequently there is a presentation of all procedures done in order to characterize a material from a mechanical and a chemical point of view.

In the first part are shown the machine used to produce the parts and the heat treatment done to improve mechanical properties.

In the second part all data collected in the test mentioned above are reported and a brief explanation of how different heat treatments produce different effects on properties of material is shown. The main focus is the comparison of fatigue behavior of 17-4 PH H900 printed in MBJ and by LPFB.

In order to study fatigue behavior, it was necessary to take a tensile test to set yielding stress, elongation and to have an idea of general behavior of material (ductile or brittle).

In the end there is a final comment about the two technologies compared and what would be needed for the future to optimized the technologies.

1.2 Utilized Machine

Since MBJ is a new technology and there aren't a lot of data in literature, during this work some companies have worked with us in order to share the know-how and improve the general quality of components.

So working with different machines with different parameters it will be easier to understand how MBJ works, what are their most critical defects. In MBJ world the leading company is Desktop Metal that in the last years has bought its principal competitor (Ex-One).

Other machine manufactorers are ITP, GE, Digital Metal.

MBJ Machine: Shop system by DM

Figure 1: Shop system by DM [1]

In the figure above a printer of shop system of MBJ is represented , then following the MBJ process, the green is put in the curing oven in order to solidify the binder and prepare the green to depowdering. (see paragraph 2.3)

Figure 2: Curing oven and depowdering station [2]

As the last step the parts are put in the furnace, where the sintering process happens

Figure 3: Furnace [2]

X25Pro

X25Pro
Desktop Metal

Figure 4: X25 Pro [3]

The X25Pro is a mid-volume advanced binder jet 3D print system that is already being used globally for the production of metal, ceramic and composite parts. Launched in 2020. It's suitable for research, prototyping, rapid product development, short-run production or continuous 24/7 production.

LPBF: M290 from EOS

EOS M 290
EOS M 290

Figure 5: EOS M290 [4]

EOS M290 is a laser printer, see EOS website [4] for technical details.

1.2 Heat treatment

Often, in Additive Manufacturing, thermal cycles are used to improve mechanical properties.

In particular for 316 L and 17-4 PH a HIP treatment is used: a high T and high-Pressure cycles in order to reduce the closed porosity of part (one of the big problems of powder technologies) and increase the density.

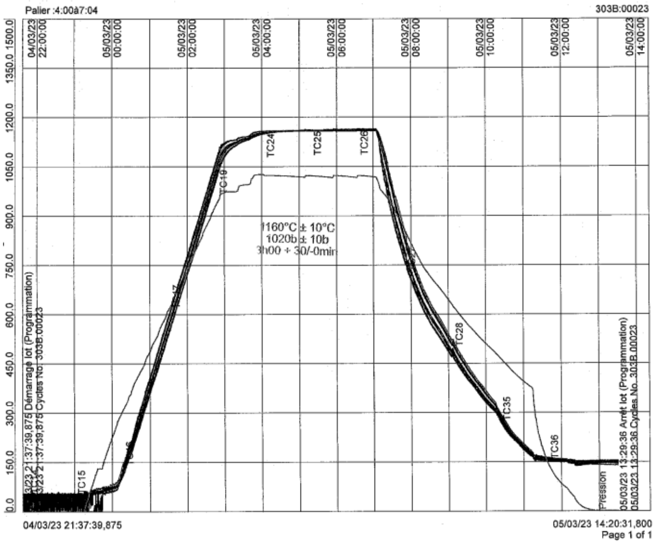

Figure 6: HIP treatment

Now considering 17-4 PH with a thermal cycle it is possible to increase a lot mechanical properties with a H900 cycles compose by two subcycles (solubilization + aging)

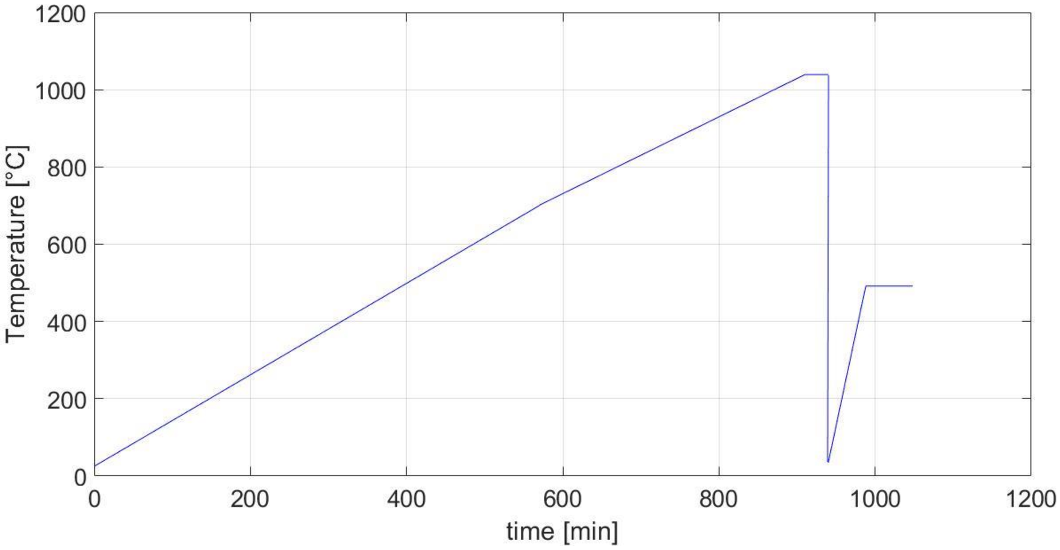

Figure 7: H900 thermal cycle

In the first part the material is solubilized and a small amount of particles of Cu are in solution, then with a strong cooling they remain blocked out of the structure. And with aging they migrate to contour of grains and increase their dimension, in this way the hardness increases.

1 General Characteristic of AM

Additive Manufacturing process is a technological technique where the part is produced adding material layer by layer, this is very different from a traditional production method, where the parts come from foundry and then to obtain its final form can undergo a forge process or stock removal process.

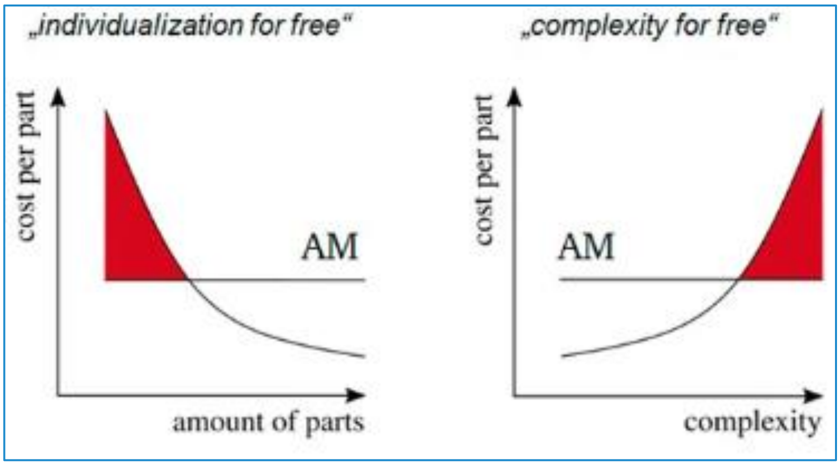

Figure 8: trend N part vs cost per part [5]

Thanks to this process we can add material only where the part requires specific stress resistance properties, so an important part is also topological optimization, where studying the load on part it's possible to redesign the part with less weight.

Another great advantage is that the cost per part does not account for complexity (as it happens with conventional technologies). These characteristics make AM perfect for a small/medium production of complex parts.

Following ASTM F2792 AM technologies are divided into 7 categories:

1. Binder jetting
2. Directed energy deposition
3. Material extrusion
4. Material jetting
5. Powder bed fusion
6. Sheet lamination

7. Vat photopolymerization

In this thesis I will focus only on Binder Jetting and Powder bed fusion technology.

Different technologies have different mechanical properties, different costs, different available materials, different print volumes and different production times; but there are some characteristics common for all AM technologies:

Pre-processing files, Orientation building, support for particular geometries, staircase effect, post-processing action.

1.1. Pre-processing file

Each AM technology needs a particular input file in order to communicate with Printer and start the job.

Always it is needed a CAD file from which we have the geometry to realize. Ending the modelling CAD software discretizes the part with a triangular mesh (the operator can decide the dimension of triangles in order that the resolution of the mesh is higher than the Machined used to avoid geometrical errors) and the output of this process is a *.stl* file.

Checking the mesh is a very good procedure because not always CAD can generate a mesh without errors. Most common errors are missed triangles, overlapping triangles and normal inverted triangles.

There is software (for example Magics) to work with stl file that can generate/delete triangles, filter the surface and refine the mesh in order to obtain a better-quality geometry and lighter file.

In addiction this type of software can split the part layer by layer in order to provide to the printer the geometry to print layer by layer.

1.2. Orientation building

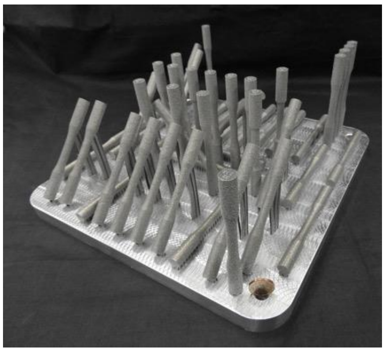

Figure 9: Oriented specimens[5]

Each technology requires a precise choice of building orientation because it affects the production time, geometry quality and the probability of having defects during printing.

Usually, orientation takes care that each transversal section must differ for previous one not too much, and since the transversal section is fixed by geometry it's possible to minimize the difference between two consecutive layers with an appropriate building orientation.

Another parameter to consider is that metal thermal shrinkage depends on the orientation of part and for the BJ the scale parameters are different for each direction.

1.3. Supporting

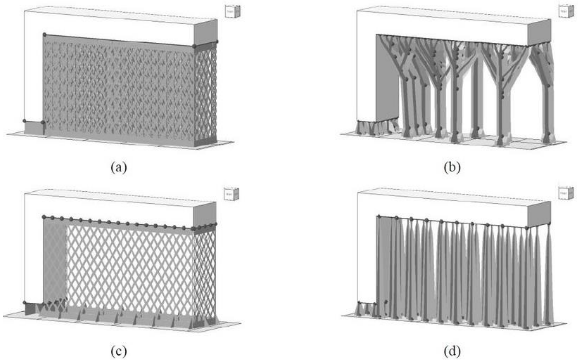

Figure 10: different types of supports [6]

Support generation is an important part of the creation of the job. In LPBF supports are fundamental because for overhang geometry in this technology a layer cannot be suspended on the powder but requires a sub structure until its geometry is completed.Moreover supports contribute to thermal dissipation during melting.

The choice of 3D geometry of support is done with a tradeoff between the material used and the stiffness of structure.

Infact all material used for them is waste and the support removal is a post processing operation that takes time and money, usually they are cut by EDM (Electrical Discharge Machining) at some height starting from the building plate, and then removed by hand from the part.

With MBJ technology the supports are not required for increasing the stiffness of structure during printing, but they are used during sintering to avoid the deformation of overhang zones of parts. Supports are not attached to the part but they are setters.

1.4. Staircase effect

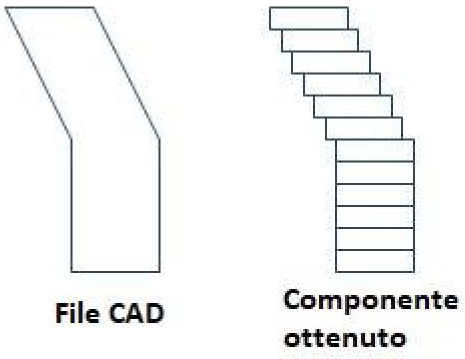

Figure 11: Staircase effect

For its definition AM builds a part layer by layer and for this reason it’s impossible to obtain perfect curvature of part but only a step geometry. This problem is reduced when thickness of layer decreases.

And here is important also the normal direction of curved surface respect to building direction.

1.5. Post-processing

Each AM technology, except for particular cases, needs extra processing after printing.

The most common are heat treatment, machining by stock removal, stress relief and support removal, sandblasting.

Heat treatments usually are done to enhance mechanical properties such as yielding point, toughness, stress max (H900), to reduce close porosity (HIP) or enhance surface hardness and corrosion resistance.

Machining by stock removal is needed when the part is "near net shape", so the main structure is completed but if are required specific tolerance for specific coupling extra machining must be done.

Stress relief is done before the support removal in order to relax the stress between the plate and the parts.

2 PBF and MBJ

In this work it will be present the comparison between three different processes all of which are under the classification of Powder bed fusion.

These processes consist in spreading powder uniformly for each layer with a roller and then an external source (Laser, electron beam) melts or keeps united only the selected material for each layer.

And this process is repeated until the part is completed. For each layer the feed piston goes up and the build platform goes down.

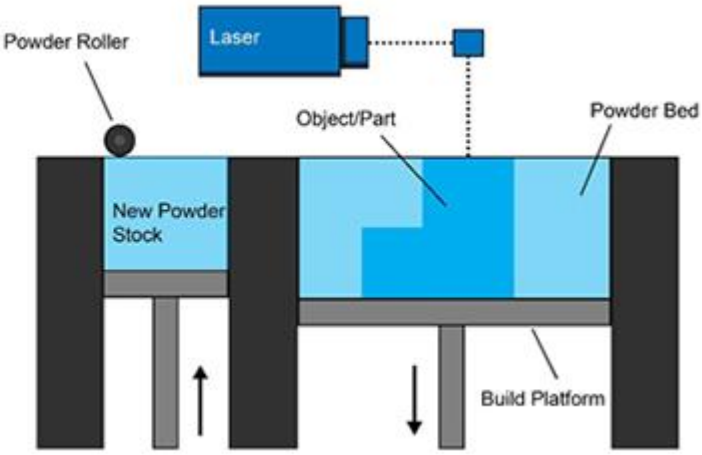

Figure 12: pistons system [7]

On this type of process there are a lot of parameters to consider that act on the final part. In particular they can be summarized in:

- Energy related
- Temperature related
- Scan related
- Powder related

The most important aspect will be analyzed in subsequent paragraphs.

Depending on which source is used there are different types of processes:

- Selective Laser Melting (SLM) of Laser Powder Bed Fusion (LPBF
- Electron Beam Melting (EBM)

All of these technologies have as feedstock powder, produced with particular techniques.

Typically, powders are produced in 2 ways:

- By gas atomization
- By water atomization

Both methods consist of interrupting liquid metal with a fluid to create spheroidal particles.

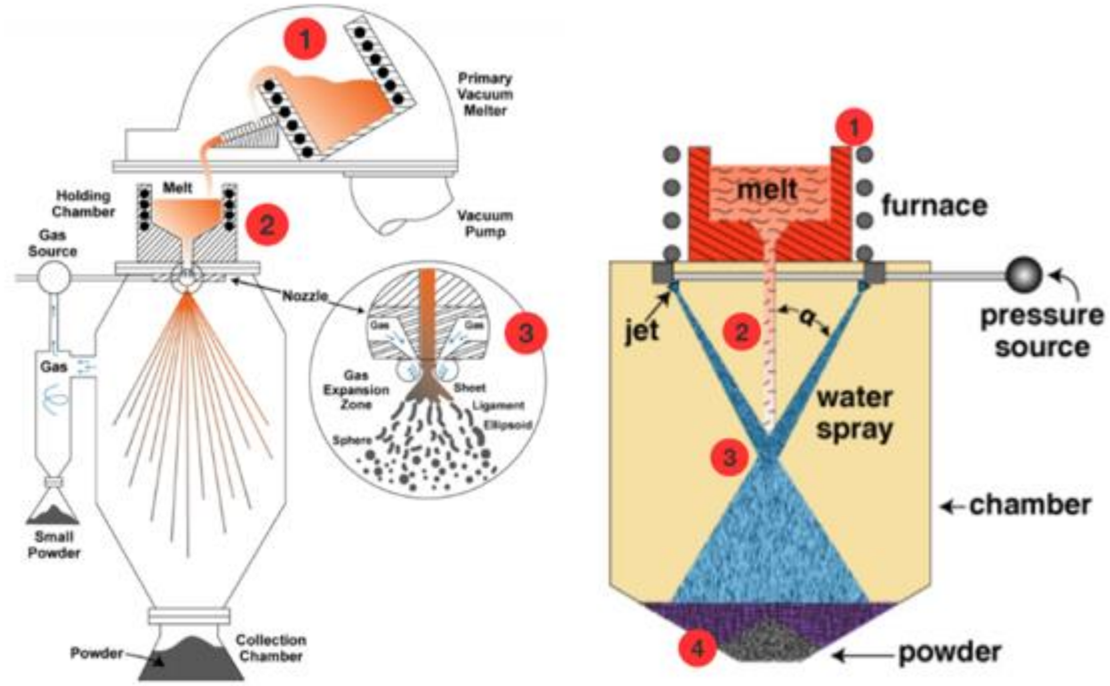
1
Primary Vacuum Melter
Vacuum Pump
Holding Chamber
Melt
2
Gas Source
Gas
Nozzle
3
Gas
Gas
Gas Expansion Zone
Sheet
Ligament
Ellipsoid
Sphere
Small Powder
Powder
Collection Chamber
1
melt
furnace
jet
2
α
pressure source
water spray
3
chamber
4
powder

Figure 13: Gas atomization on the left and water atomization on right [8]

In gas atomization the melted metal is injected by orifice and then hit by gas, then the particles cool and condensate, then for gravity the coarse powder are collected in a container down of machines, instead the small particles are collected by a channel in the middle of room.

In water atomization the pretty same thing happens but then the powders need a drying process. And since the pressure of water is very high, here the process is rawer. So, a powder produced in gas atomization layer has a better quality.

2.1. LPBF

LPBF is an AM technology that uses a laser to melt layer by layer the powder of various metal material. Nowadays there are a lot of machines available for this technique: for examples there are EOS, Renishaw, SLM Solution and Concept Laser.

The principal issue of this is to have good control of laser system, the higher is the laser power, the faster is melting and shorter lead time. Today, some equipment manufacturers commercialize the system with multiple lasers allowing speeding up manufacturing process.

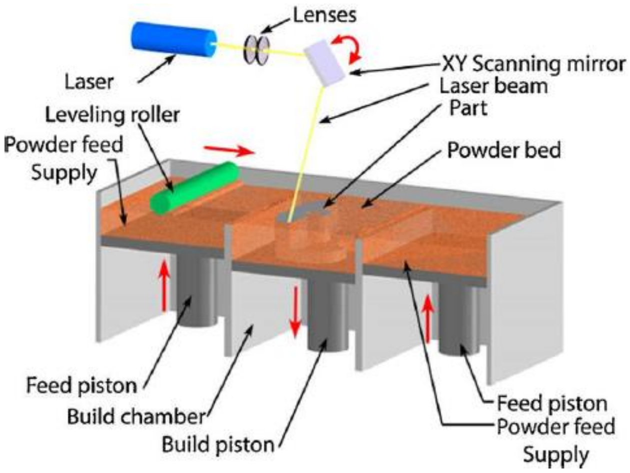
Lenses
Laser
XY Scanning mirror
Laser beam
Part
Leveling roller
Powder feed
Supply
Powder bed
Feed piston
Build chamber
Build piston
Feed piston
Powder feed
Supply

Figure 14: pistons system [5]

The layer thickness of these part usually is between 30-60 µm but can range up to 80 to speed up the process.

The job is done in an inert atmosphere or in vacuum in order to prevent oxidation of the metal part and preserve a good chemical composition.

A big problem of this technology is that due to a great amount of energy the material need support both to overhang part and to improve the heat exhange in order to prevent deformation of final part.

Since the big thermal gradient usually presents non negligible residual stresses and for this reason it's a common use to consider a post-processing thermal cycle of stress relief.

Another limit of this technology is the presence of support. In fact, all of these parts need to be supported over the built plate and the removal part of support is the slowest part of this process, as it is generally made by hands, and requires a lot of experience to design it correctly.

2.2. EBM

Electron Beam Melting is a process where the part is created melted layer by layer by electron beam, for this the machine needs to be in vacuum, otherwise the beam can ionize the particles, and this can create serious damage. In addiction the process is done after a pre-heating passage in order to have less residual stress and to improve the desorption of gases and limit the oxidation of components.

The layer thickness is about 50-200 µm, in other words this a faster machine respect to LPBF, but with a lower resolution and higher component surface roughness.

Another difference respect to LPBF is that here the powder is semi-sintered, because the high energy beam can charge the particles and since the work room is in vacuum condition the particle can rise up and produce a very bad resolution of component.

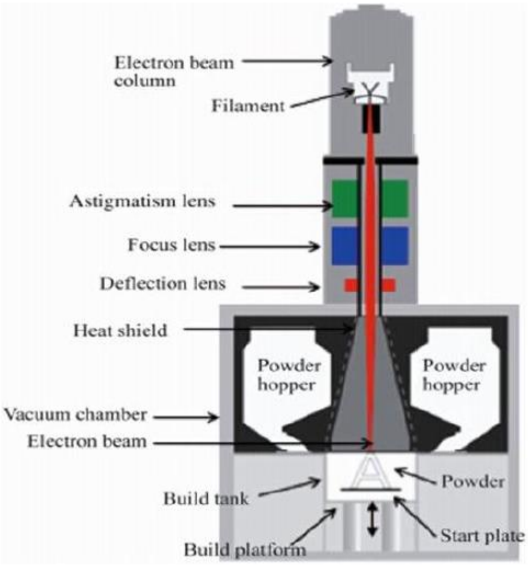
Electron beam column
Filament
Astigmatism lens
Focus lens
Deflection lens
Heat shield
Powder hopper
Powder hopper
Vacuum chamber
Electron beam
Build tank
Powder
Build platform
Start plate

Figure 15: Electron Beam melting [5]

In conclusion, EBM is faster, but produces components with higher roughness and poorer surface finish.

2.3. MBJ

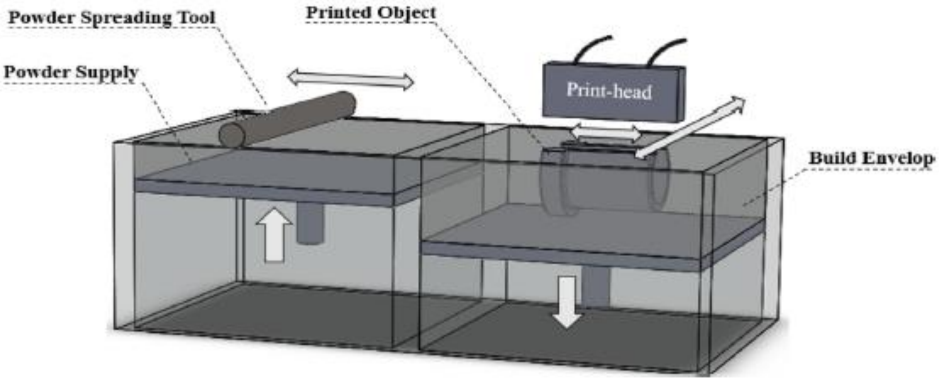
Powder Spreading Tool
Printed Object
Powder Supply
Print-head
Build Envelop

Figure 16: Metal Binder Jetting [7]

Binder jetting is a different process from the previous two, since doesn't use a source of heat to build up the component but a binder, that must be carefully chosen with respect to the material that is used in order to improve the good matching between the binder and the powder (the binder is a water based organic solution).

The process consists in a spread of metallic powder layer by layer and then the binder is put selectively in order to fix the component. The outcome of this printing phase is called “brown”, the parts remain in the building box and cannot be handled as they are very fragile.

The second step is called curing: in this process the building job is put into an oven in which it is subjected to a heat treatment where the temperature has a ramp profile in order to dry the binder and to cure it, so it is possible to fix the geometry of the component and have a part, still fragile, but handable. The part now is called “green”.

The third step is the depowdering: the part is put in depowering station, a workroom dedicated to containing the powder’s dispersion, and here the operator starts to clean all parts with specific tools based on principle of separate the parts from the unbinded powder. This process is at the state of art the most manual and the slowest of the cycle, but many studies are working in progress to automize this.

The third step is called debinding and sintering: the green parts are put in an oven where they are subjected to a thermal cycle in order to evaporate the binder and then the oven increases the temperature in order to sinter the part. Here the component is subjected to a relevant shrinking of 20/30 % in volume, in fact the most critical part in BJ is to design a good geometry taking into account the deformation phenomena occurring in sintering cycle. Here the density increases a lot, and the material assumes the final mechanical characteristics.

The process is very sensitive with respect to a lot of parameters (binder saturation, layer thickness, material, spreading profile, design of pattern of different region: shell, inner shell, top, bottom) and for this reason it requires a lot of experience and a lot of work on data available.

The layer thickness is about to 30-200 μm [8]. DM systems range from 30 to 75 μm.

These three technologies are similar but also different, in particular it needs to be considered a different design rule to optimize the process for the single part.

The aim of this thesis is to analyze mechanical properties of two stainless steel alloys for AM (316L and 17-4 PH, both in LPBF and MBJ) and how they improved after thermal treatment.

With respect to MBJ, due to the manufacturing process the parts suffer of porosity defect that decreases consistently the mechanical properties with respect to conventional manufacturing techniques.

In particular the studies show that heat treatments like H900 and HIP improve a lot the mechanical characteristics and also the density, arriving near to 99% [8] of material.

2.4. MBJ vs LPBF process

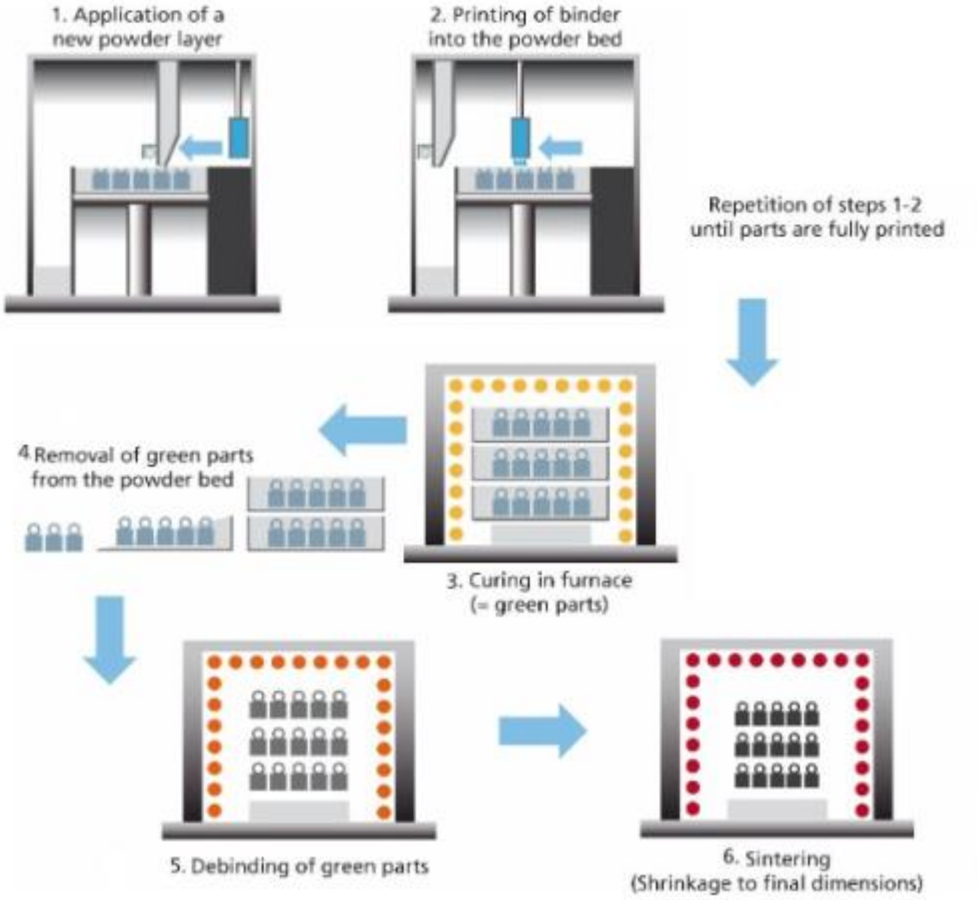
1. Application of a new powder layer
2. Printing of binder into the powder bed
Repetition of steps 1-2 until parts are fully printed
4 Removal of green parts from the powder bed
3. Curing in furnace (= green parts)
5. Debinding of green parts
6. Sintering (Shrinkage to final dimensions)

Figure 17: Metal Binder Jetting process

The main difference between two process is that the MBJ is a multi-machine process, where the printing is faster respect to the analogous of LPBF.

In fact, to obtain the final part MBJ need 4 different machines (printer, curing oven, depowdering station, furnace); on the other hand, LPBF need only two processes (printer and supports removing).

It's difficult to say what process is faster because is very part-dependent and for each different geometry need to do different considerations. In fact, for the LPBF the slowest part is the printing process, instead for MBJ the slowest part is the depowdering the green part.

3 Powder characterization

The powder is characterized by a PSD and flowability.

In MBJ the density of powder directly influences the density of green part that is directly linked to final accuracy and quality of parts!

Another important topic is the reusability of power in order to improve efficiency and reduce pollution.

Between MBJ and LPBF there are some differences on how to deal with powder:

- In LPBF, all of powder exceeding the job are sieved inside the printer, and this powder may have a bit lower characteristic because the original distribution of particle can change. A good standard is doing a periodic chemical/physical analysis after 10/20 recycling.
- In MBJ, since the powder is collected both from recycling to see if the property are exceeding one from printer and after depowdering, there is a possibility that some particle of binder remains in the recycled powder, it's been chosen that after recycling an amount near 20/30% of virgin powder will be added in order to try to maintain the original composition.

3.1. PSD

PSD stands for Powder Size Distribution; it represents the distribution of diameter of particles.

Usually, this value is obtained by Image Analysis, obtained with SEM, and post processing that analyze the image and for each particle return its diameter and then with simple mathematics it's possible to have the histogram of particles

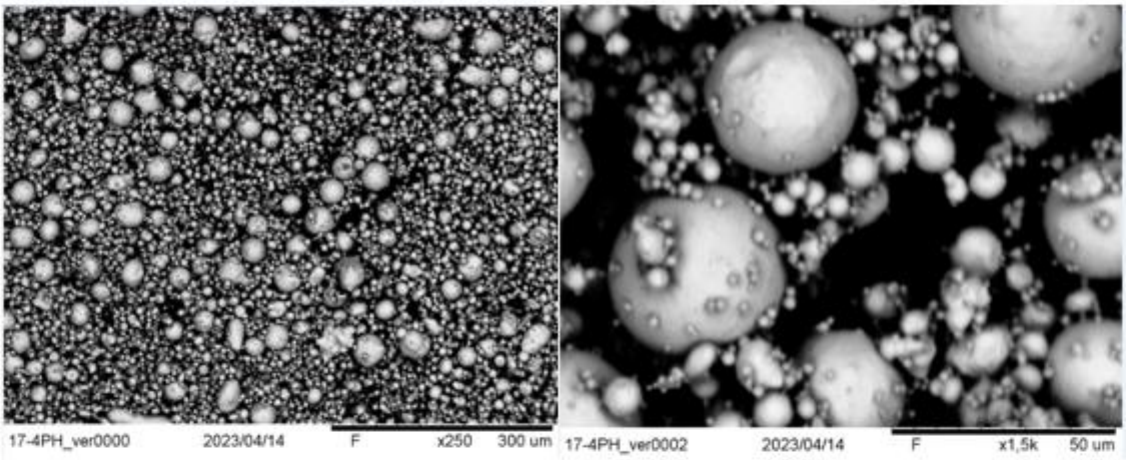
17-4PH_ver0000
2023/04/14
F
x250
300 um
17-4PH_ver0002
2023/04/14
F
x1,5k
50 um

Figure 18: Powder particle x250 and x 1500

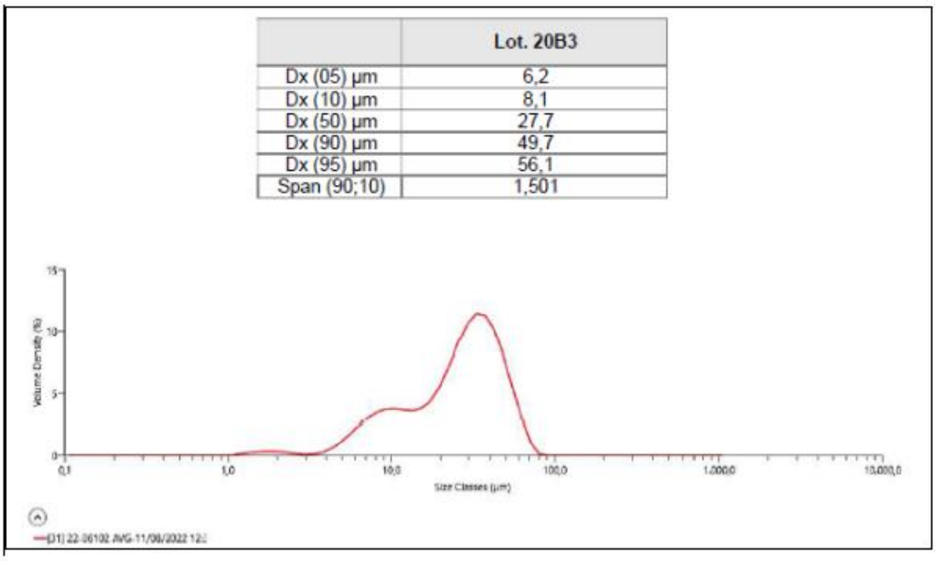

	Lot. 20B3
Dx (05) µm	6,2
Dx (10) µm	8,1
Dx (50) µm	27,7
Dx (90) µm	49,7
Dx (95) µm	56,1
Span (90;10)	1,501

Figure 19: PSD of 17-4 PH

For a good spreading of powder bed, it is important that the particle have a near spheric shape and from literature [7] it has been seen that with smaller particles the porosity decreases.

3.2. Flowability

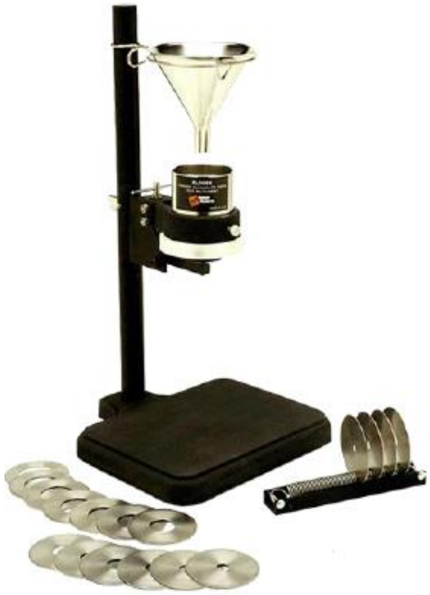

Figure 20: equipment for flowability test [9]

Flowability is an important parameter, since if the powder has a good flowability it means that it is easy to be deposited and so it is less likely to produce defects during printing.

A way to measure this parameter is the angle of repose.

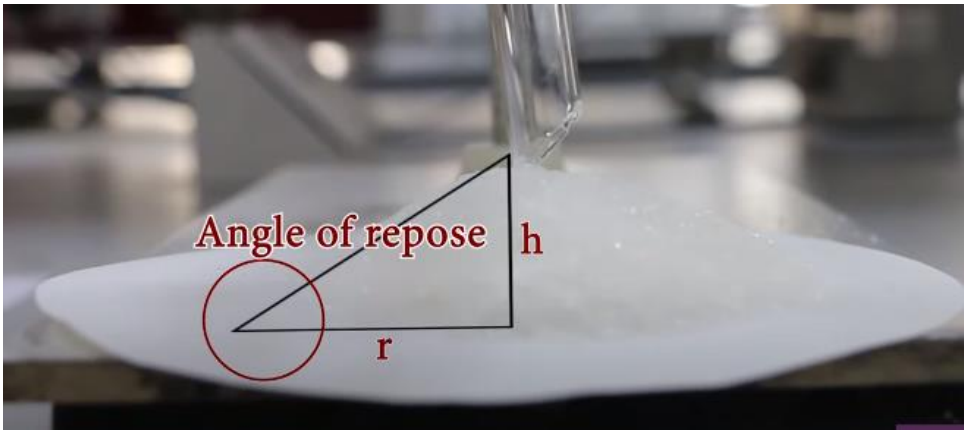

Figure 21: Angle of repose

Typically a good angle is between 25-30°.

4 Mechanical characterization of materials

This thesis has the aim to investigate the mechanical behavior of different stainless steel with different production processes (MBJ, LPBF).

First a campaign of static tests on coupons has been done to characterize the material with

- yielding stress
- elongation at break
- max stress
- Young Modulus

Then with this initial information, a fatigue campaign has been performed in order to obtain a Wohler diagram and at the end doing a fracture analysis to see if the fracture is ductile or brittle with all consequences.

4.1. Tensile test

The tensile test is done following the ASTM E8E8M where it is specified the geometry of the specimen, how to handle the machine, how to position the extensimeter.

This test consists in positioning the specimen to the grab, then, in this case, with hydraulic circuit the grabs are closed and in this way the specimen is fixed to the machine.

Whit another hydraulic circuit the grabs start to move vertically pulling the specimen, the test is done in displacement control, and the parameter is velocity of deformation.

Usually for metallic materials the curve is done in this way:

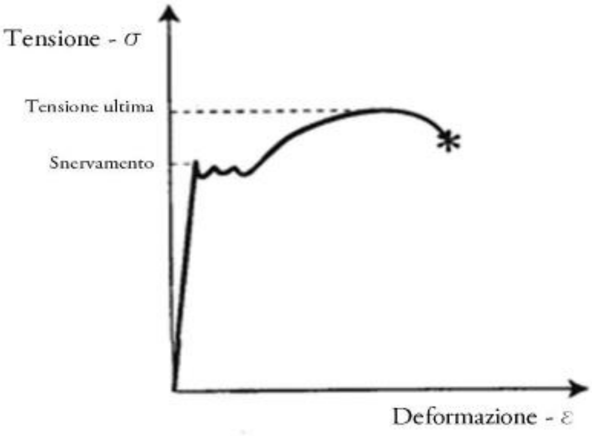

Figure 22: stress strain diagram

The typical variable in this the engineering stress and engineer strain that are define as follows:

$$\sigma = \frac{F}{A_0}$$

[1]

$$\varepsilon = \frac{\Delta L}{L_0}$$

[2]

Where F is force applied by machine, A_0 is the Area of the specimen in a non-deformable condition,

L_0 is the specimen length before starting the test, ΔL is the difference between L and L_0.

This assumption is done since during the test the length and area dimension change for plastic deformation and at the end of test A would become infinitesimal.

In the first part of the test the specimen deforms proportionally to the force applied by machine, from the data coming from extensimeter it can be obtained E, elastic Modulus of the material, as the slope of linear part of curve.

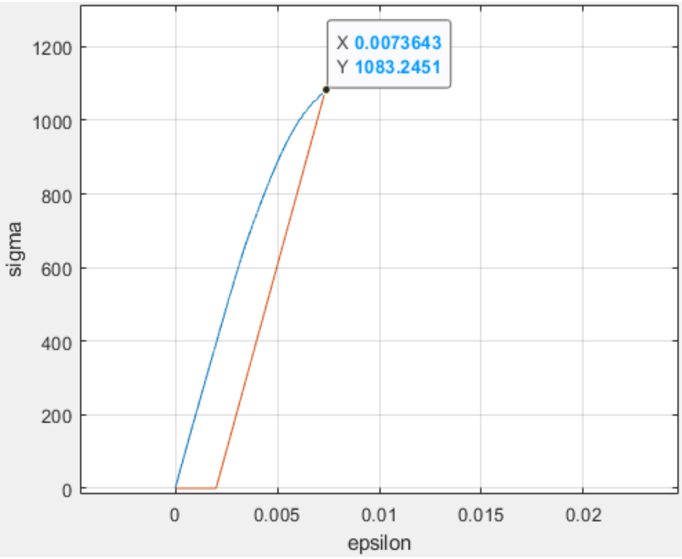

Figure 23: find Rp 02

The second step is to obtain the sigma Yielding: usually to obtain this value the definition is when the material deviates more than 0.2% from elastic behavior (R_{p02}).

The last important data coming from tensile test are the σ_{uts} , ultimate tensile stress, that is the max stress that material can withstand during the experiment and elongation, max length that specimen reach compared to its initial length.

An important parameter to be considered is the deformation rate, defined as:

$$\frac{d}{dt}\varepsilon = \frac{d\left(\frac{L-L_0}{L_0}\right)}{dt} = \frac{1}{L_0}\frac{d}{dt}L = \frac{v}{L_0} \qquad [3]$$

For metal material if $\dot{\varepsilon}$ increase also mechanical resistance increases. During the test typically in elastic domain the deformation rate remains low, in order to better catch the elastic response of material, then when material starts yielding the deformation rate can be increased to reduce the time of test.

4.2. Density measure

Density is an important characteristic of each structural component because it has a direct impact on weight and can give us other information such as porosity and corrosion resistance. In LPBF and MBJ, where the process starts from powder the density is important as key parameter.

Usually [6] density measure is done using "Archimedes principles", where it's used the thrust of water to find the density.

The test consists in 2 measures: the first is a classical measure over the scales, then resetting the instruments, the sample is remeasured submerged in distilled water. The ratio between these two measures represents the density of metal.

Measure 1: the weight of metal part in air $M_1 = \rho_m g V$ [4]

Measure 2 : the weight of part in water $M_2 = -\rho_w g V$ [5]

In the end: $\rho_m = \frac{M_1}{M_2}$ [6]

Doing this experiment some assumptions are done:

1. The density of water is considered as it is at T=20 °C
2. The bubble of air on surface of piece are neglected and not considered for measures (the operator needs to take care of positioning in a proper way the metal pieces in order to avoid the bubble
3. The density of air, and as consequence its thrust is not considered for the measures.

In case we want to consider also this factor, it's necessary to know the density of air and consider in each measure the density of air.

It becomes:

$$M_1 = \rho_m g V - \rho_{air} g V \quad [7]$$

$$M_2 = -\rho_w g V + \rho_{air} g V \quad [8]$$

And from this two:

$$\rho_m = \frac{M_1}{M_2}(\rho_{air} - \rho_w) + \rho_{air} \quad [9]$$

4.3. Fatigue test

During the last two centuries, a lot of unexpected failures of machine components and structures have occurred, even if the applied stress was much lower than the static limit of the employed materials. However, these components were subjected to time-varying stresses.

Intuitively, in most cases the loads affecting the structures are not constant, but they have a variable amplitude. This amplitude depends on several factors: machine operation, environmental conditions etc.

a. Vehicle axes
b. Pressure in a nuclear reactor
c. Car wheel
d. Bending in a rolling mill
e. Mechanical joint
f. Acceleration of military aircraft
g. Pipeline pressure
h. Acceleration of civil aircraft

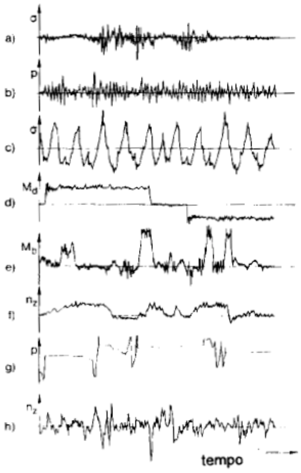

Figure 24: different type of fatigue cycles

The fatigue phenomenon refers to the decreasing of the strength because of the time-varying applied loads. The change in the material strength could cause the nucleation of micro-fractures (cracks). These cracks could propagate in time due to the variable load and produce the failure of the component, even if the applied stress is much lower than the Ultimate Tensile Strength.

The test tries to reproduce the load condition following the ASTM E466.13432.

The most common load conditions are:

- Traction- compression
- Alternating bending
- Rotating bending

In this thesis the test is a constant amplitude one but are possible also other types of tests.

4.3.1. Definition of fatigue cycles

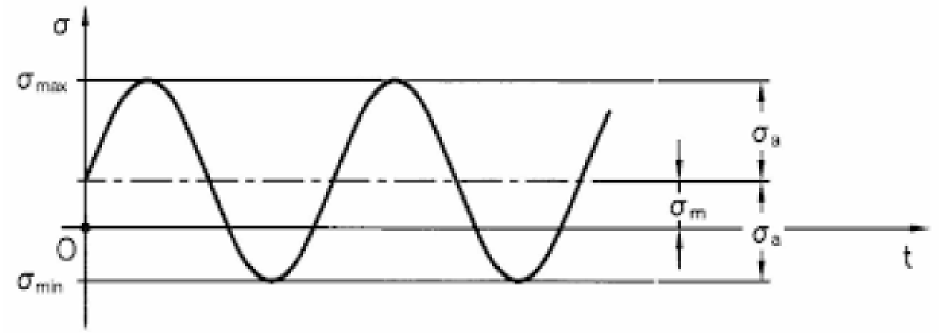
σ
σ max
σ a
σ m
O
σ a
σ min
t

Figure 25: Alternate fatigue cycle

To completely define a fatigue cycle are need:

- Frequency of oscillation
- Sigma max amplitude

[10]

The fatigue limit usually is defined as maximum value of the alternating cycles.

Other important variables are:

- $\sigma_{mean} = 0.5 \cdot (\sigma_{max} + \sigma_{min})$ [11]
- $\sigma_{alt} = 0.5 \cdot (\sigma_{max} - \sigma_{min})$ [12]

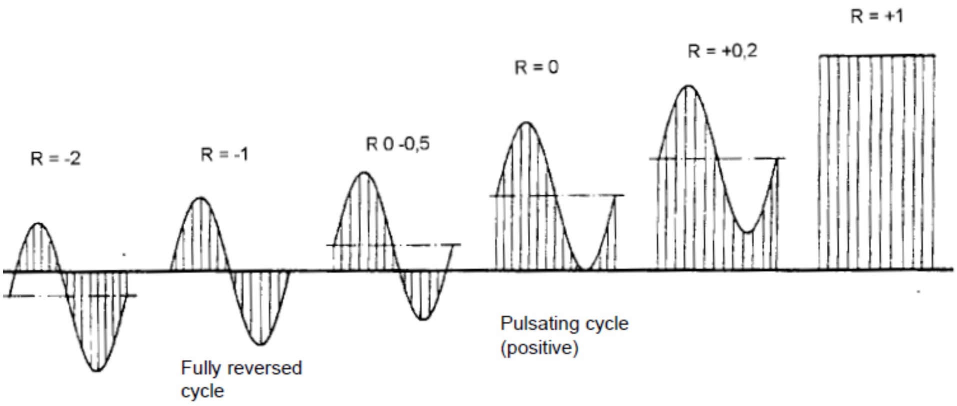
R = -2
R = -1
R 0 -0,5
R = 0
R = +0,2
R = +1
Fully reversed cycle
Pulsating cycle (positive)

Figure 26: different cycles respect to R

If R changes, change the ratio between σ_{mean} and $\sigma_{alternate}$ and this has a big impact on the result in principle since the mean stress change changing R.

4.3.2. Wohler diagram

A typical diagram to correlate $\sigma_{alternate}$ and number of cycles to failure is the wohler diagram

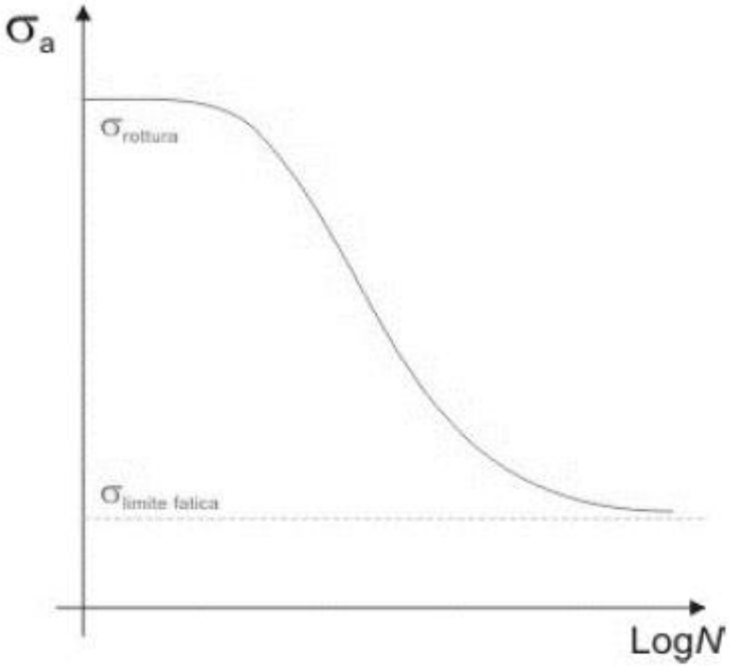

Figure 27: typical fatigue curve

The diagram shows that for low Number of cycles material resists about σ_{max} , then about 10^4 about and 10^7 cycles presents a linear behavior, and usually for steel and Fe alloy it's a $\sigma_{fatigue}$ that is about 0.5 σ_{max}.

4.3.3. Statistical method for evaluating fatigue limit

Results of fatigue, for their nature, present a statistical behavior for 3 main reasons:

- Material Heterogeneity, due to technological process and presence of inclusion or defect
- Preparation of specimens that possibly can introduce defect during mechanical machining or heat treatment.
- Uncertain of measure, load applied, machine placement and so on

As consequence for a σ on Wohler diagram does not correspond a single value of N, but a distribution of rupture that follow its statistic.

So, the correct interpretation of the diagram is:

For each value of σ the specimen can break following a distribution, from literature [15] It was observed that a log normal distribution follows well the trend of events.

In this way each curve represents an equiprobability curve of rupture of specimen. Usually, the Wohler curve is built as 50% probability of rupture.

This implies that a linear interpolation of result doesn't take into account this consideration because each data has the same weight on result, that is wrong for two main reasons:

- Run out sample have a different meaning respect to a break one
- Since the data belongs to a distribution is not properly correct compare different data for different stress level that represent different percentile

Method used in this thesis is the Maximum Likelihood method,

That consists in a method that starts with some data and a probability density function (in our case a log normal distribution) and maximizes the parameter of distribution for having a bigger probability we have the parameter of pdf that best fit our data.

Using formulas:

The probability of occurrence of an event I in an interval of dy is

$$P_i = f(y_i, \alpha, \beta)dy$$ [13]

Instead the probability of a specimen can survive respect a run out is

$$P_i' = 1 - F_i(y', \alpha, \beta)$$ [14]

The total probability of my campaign is:

$$L(\alpha, \beta) = \Pi_i f(y_i, \alpha, \beta) \times \Pi_i\big(1 - F(y_i, \alpha, \beta)\big)$$ [15]

Appling logarithmic to simplify calculus:

$$\ell(\alpha, \beta) = \sum_i \ln\left[f(y_i)\right] + \sum_j \ln\left[1 - F(y_j')\right] + n \cdot \ln(dy)\,.$$ [16]

4.3.4. Staircase

If the ML is used to characterized Wohler diagram, there is another method to evaluate the limit of fatigue for a certain Number of cycles. This method is called Dixon and Mood Method or staircase method. Usually [16] for each test it needs to have 15 or 20 samples, but some studies proved that results are significatively also with 5 samples[17].

The method consist in starting with a possible value of fatigue limit σ_0 for which we are sure that simple will go at run out, then choosed an increment $\Delta\sigma$ to test the simple at higher stress level.

The execution of test is done in this way:

Testing first sample, if it goes to run out the stress level is incremented, otherwise stress level is decreased by $\Delta\sigma$. At the end of samples, it starts the count from which it's possible to obtain the statistical parameters.

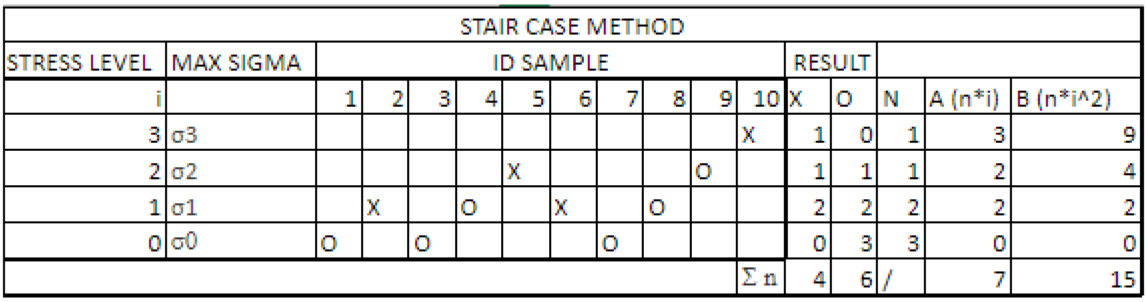

STAIR CASE METHOD																
STRESS LEVEL	MAX SIGMA	ID SAMPLE										RESULT				
i		1	2	3	4	5	6	7	8	9	10	X	O	N	A (n*i)	B (n*i^2)
3	σ3										X	1	0	1	3	9
2	σ2					X				O		1	1	1	2	4
1	σ1		X		O		X		O			2	2	2	2	2
0	σ0	O		O				O				0	3	3	0	0
											Σ n	4	6	/	7	15

Figure 28: typical Stair case

Looking at the figure, it represents a scheme of 10 stencils to obtain a fatigue limit.

Where X means rupture and O run out. At the end of test, the least numerous event between X or O is consider calculating parameter A and B, useful to obtain fatigue limit.

$$\sigma_{D_{50\%}} = \sigma_0 + d\left(\frac{A}{N} \pm 0{,}5\right) \qquad [17]$$

Where sigma D represents the stress level at which the probability of rupture is 50%.

If run out is more frequent event it will take + otherwise -.

This method can estimate also the standard deviation as

$$s = 1{,}62d\left(\frac{(NB-A^2)}{N^2} + 0{,}029\right)$$

[18]

An empirical rule to evaluate if this method is appropriate or not is the following:

$$\frac{(NB-A^2)}{N^2} < 0.3 \qquad [19]$$

4.4. Specimen geometry and preparation

The specimen geometry has fundamental importance since for each geometry the stress can concentrate in a different way and the final result could be influenced. In addiction, if the dimension of diameter changes, the scale effect on specimen change, both for fatigue and static test.

The ASTM E8M8 gives precise dimension for each diameter to test.

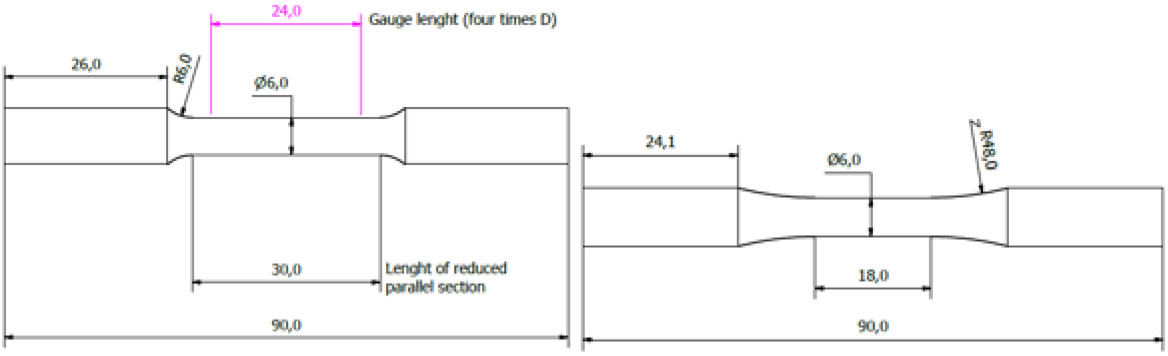
24,0
Gauge lenght (four times D)
26,0
R6,0
Ø6,0
30,0
Lenght of reduced parallel section
90,0
24,1
Ø6,0
R48,0
18,0
90,0

Figure 29: Geometry of tensile specimen and fatigue specimen

Choosing a diameter test of 6mm the geometry is the following.

Since MBJ system used to prepair the samples for this thesis has a limit of height, our specimens have length of 85 mm, as it changes only the length of grabbing, if it will be enough to correct execution of test this parameter doesn't affect the measure.

The specimens of MBJ are obtained from hexagonal profile in order to position them properly during sintering. Instead, LPBF specimen had a cylindrical geometry.

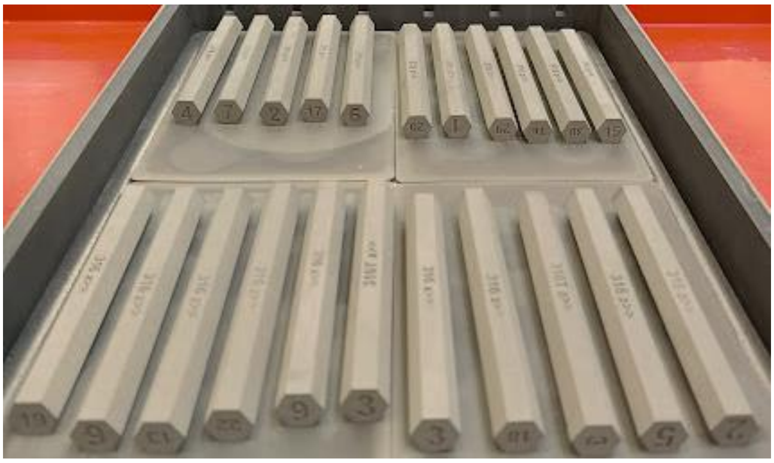

Figure 30: Furnace retort

Then specimens were machined by lathe. Since for fatigue roughness is an important factor, as usual the machining has been planned to have a first part of roughing and a second part of finishing in order to obtain a Ra of 0.5 μm.

5 Chemical characterization of materials

5.1. 316L austenitic stainless steel

316L	
Cr	16.00-18.00 %
Mn	Max 2.0%
C	Mac 0.03%
Si	Max 1.0
Ni	10.00-14.00 %
S	Max 0.03%
P	Max 0.04%
Mo	2.00-3.00 %
Fe	Balance

316L is a typical Austenitic Stainless steel, whitch characteristic is to have a very good anticorrosion properties, and being stainless Steel have good mechanical properties.

It's used in the food industry, Aerospace/Turbine industry, chemical environment, but Parts are not ideal in temperature range 427°C - 816°C where precipitation of chromium carbides occurs.

Typically, it is divided into 316 L and 316, where the difference is that in 316L its present less Carbon (L stands for Low carbon) and so 316L has better corrosion properties and is better for welding.

5.2. 17-4 PH martensitic stainless steel

17-4 PH is a martensitic stainless steel, used in structural engineering due to its good corrosion resistance and very good mechanical properties.

For this thesis and for Aeronautical field 17-4 Ph are more interesting.

17-4PH	
Cr	15.00-17.00%
Mn	Max 1
C	Max 0.07%
Ni	3.0-5.0%
S	Max 0.03%
P	Max 0.04%
Nb/Ta	0.15-0.45%
Cu	3.0-5.0%
Mo	Max 0.30%
Fe	Balance

6 Parameter definition

In this paragraph it will be specified that all variables are labelled and tracked.

6.1. Aidro by Desktop Metal - MBJ

Starting from Aidro's MBJ specimens: each job has its own print order, where it's possible to track following machine parameters (printing phase):

- Spreading profile
- Powder lot
- Saturation
- Region type and definition
- Layer height

In addiction each part and specimen are labelled in a unique way in order to have the possibility to find its position on the build box, its print direction.

In particular the

- X printed 17-4 PH specimens' job is MBJ-ODS044
- Z printed 17-4 PH specimens' job is MBJ-ODS045
- 316L printed specimens' job is MBJ-ODS046

The parameters used are standard parameter of DNV certification for Shop system [27].

DNV is one of the most important accredited registrars working mainly with Oil and Gas Industries [28].

Following the MBJ process, another documentation is the Temperature profile of sintering, but for company policy it can't be published.

6.2. Eos M290

The Eos material has been printed in M290, the material is 17-4 PH end the granulometry of powder is available on EOS datasheet, also layer thickness and all job parameters.

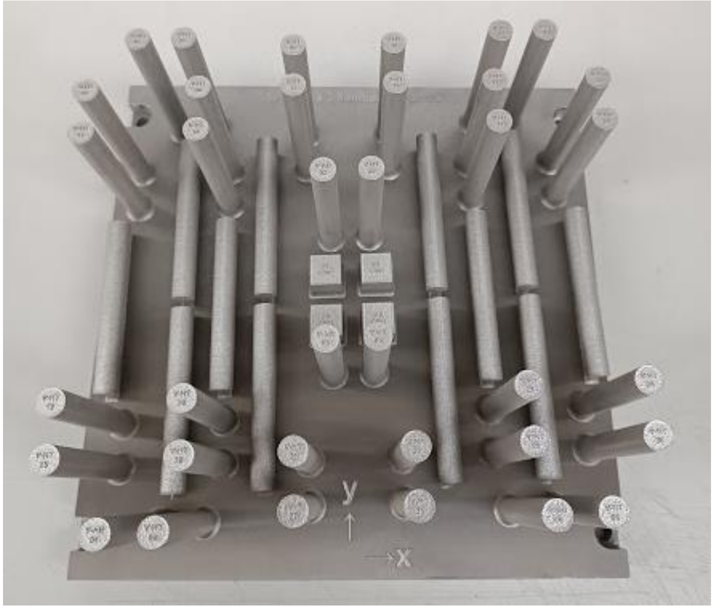

Figure 31: EOS steel plate

Then the job did a heat treatment of stress relief in atmospheric condition (as standard Eos indicates) before that the specimens have been separated from the plate by EDM

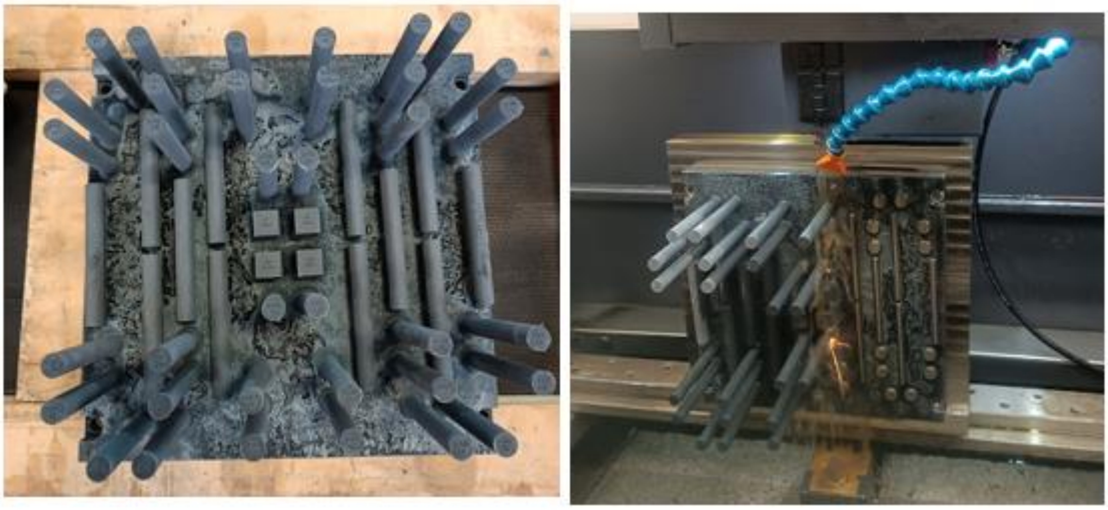

Figure 32: Steelplate after stress relief during EDM cut

7 Heat treatment

For AM components, but not only, heat treatments are a good solution to improve the mechanical properties.

In particular in Powder bed technology, where the porosity has a big impact on component, often Hipping treatment is required to close or reduce the closed porosity (open porosity are in contact with external surface).

7.1. HIP

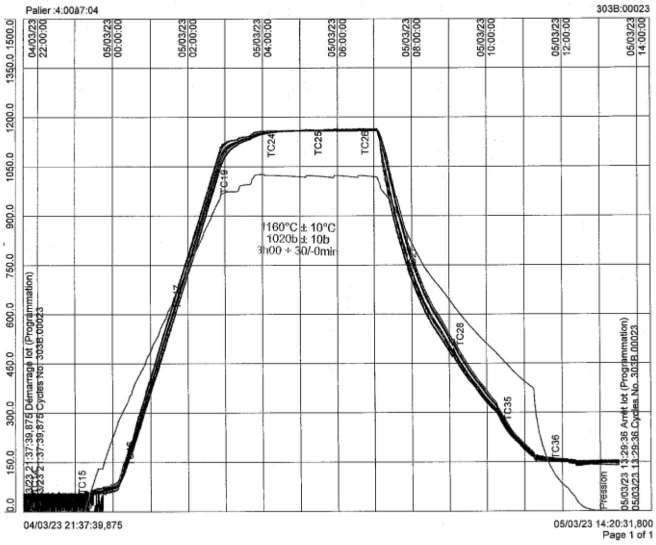

Figure 33: HIP thermal cycle

Hipping treatment is done by Bodycote, a company specialized in thermal treatment located in France, which provided the specific thermal cycles for my work, in this case the cycles is done at 1000 °C and 1000 bar for 3h!

This cycle is adequate both for 316L and 17-4 PH since the principal scope is to put the pieces in a hot and pressurized environment to force the close porosity to shrink and possibly decrease.

No chemical action is required.

7.2. H900

H900 is a hardening process in which material increases mechanical properties due to precipitation.

Not all stainless steels are suitable for this cycle, in particular only steel that have metastable phase.

For example, only 17-4 PH between the two steels chosen can do this treatment and here the mechanism that improves mechanical properties is the precipitation of Cu since when start the transformation Austenite-Martensite the solution become over-saturated and Cu exit and precipitate and generate a defect that can block the dislocation.

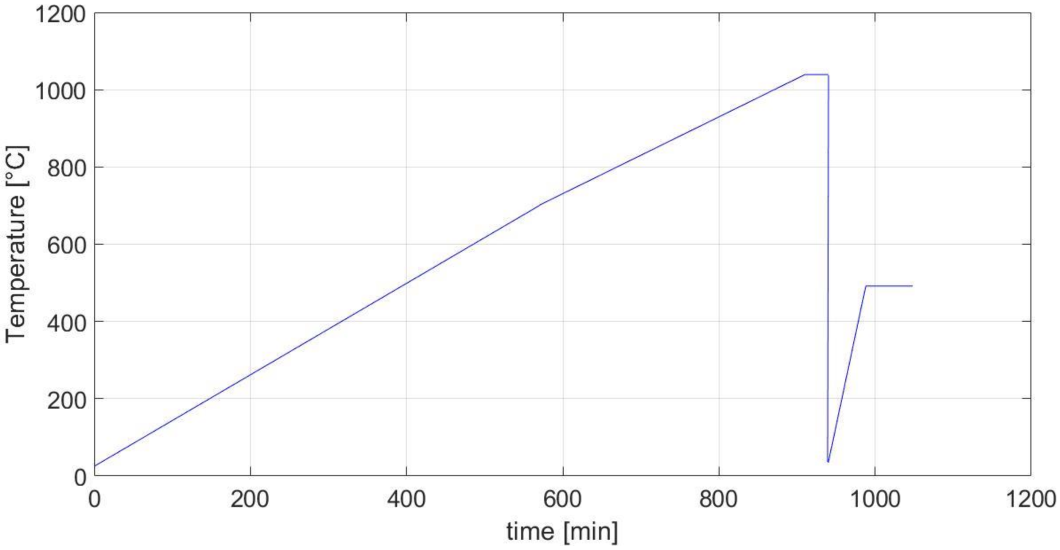

Figure 34: H900 thermal cycle

In this figure we can see a quality trend of Thermal cycle, in the first part there is a dT/dt =v1, in the second part velocity of T decreases at value v2, in the third part it presents a Maintenance of temperature, then it presents a maintenance and at the end there is aging.

Figure 35: Lab furnace

In this figure it's shown a furnace where the heat treatment has been done, in the Aerospace department of Politecnico di Milano.

8 Analysis of result

Using equipments of Aeronautical Laboratories at Potitecnico di Milano (DAER), there was the possibility to investigate mechanical properties of some AM technologies. This approach is very useful since even if 3D printing machine manufacturers made big campaign to certify their materials, with this type of production where the machines have a big number of parameters to set it is possible that optimizing its own process the mechanical characteristics change noticeably! And it was really interesting to see how properties change with variation of parameters.

For this type of work the equipments available are:

- Tensile test machine for static and fatigue conditions
- SEM
- Optical microscopy
- Lapping machine
- Cut off machine for metallographic specimens

8.1. Mechanical properties

The main scope of this thesis is to analyze how mechanical characteristics are influenced by heat treatment and how they change the physical/chemical composition.

There are a lot of configurations tested, following there will a schematic representation of all of them:

	MBJ				LPBF	
	AS BUILT	H900	HIP	HIP+H900	AS BUILT	H900
17-4 PH	X	X	X	X	X	X
316 L	X	/	X	/	/	/

All these configurations are tested from different country and company:

- Aidro provided the main part of specimen (MBJ of 316L and 17-4 PH) produced by Shop System Desktop Metal and the finishing of samples by lathe
- EOS provided the LPBF specimen (printer M290)
- Bodycote provided HIP treatment
- DAER of Politecnico di Milano and TAV Vacuum Furnaces provided the H900 treatment
- All of conditions tested in static condition are done both for X and Z direction since the 3D printing it's, for intrinsic properties, not isotropic (in properties changes sensibly respect the plane of layer and the building direction).

The general rule seen is that the critical direction is the Z direction since bound between 2 separate layers is weaker respect bound inside single layer.

All of specimens both AB (as built) and HT (heat treated) are machined by lathe machine in Aidro.

8.1.1. Tensile test

The tensile tests are done using an MTS 647 series, the velocity of deformation is 0.5 mm/min for all specimens in elastic condition, in this way the regulation is respected.

Then, for example the 316L specimens, that showed a very high elongation, the velocity in plastic condition is increased up to 3 mm/min, in this way the time of test is reduced a lot and the quality of measure remains acceptable.

Since the machine output is deformation by extensometer (in elastic condition), total length and force by machine to obtain the stress-strain diagram each specimen diameter is measured to have stress level.

From tensile test is possible to obtain interesting information:

- E: Young Modulus from stress and strain by extensometer in elastic condition
- σ yielding as Rp 02 define as the σ level at which the behavior differs from elastic one of 0.02%
- σ max
- Elongation (strain): maximum level of displacements before rupture divided by L0

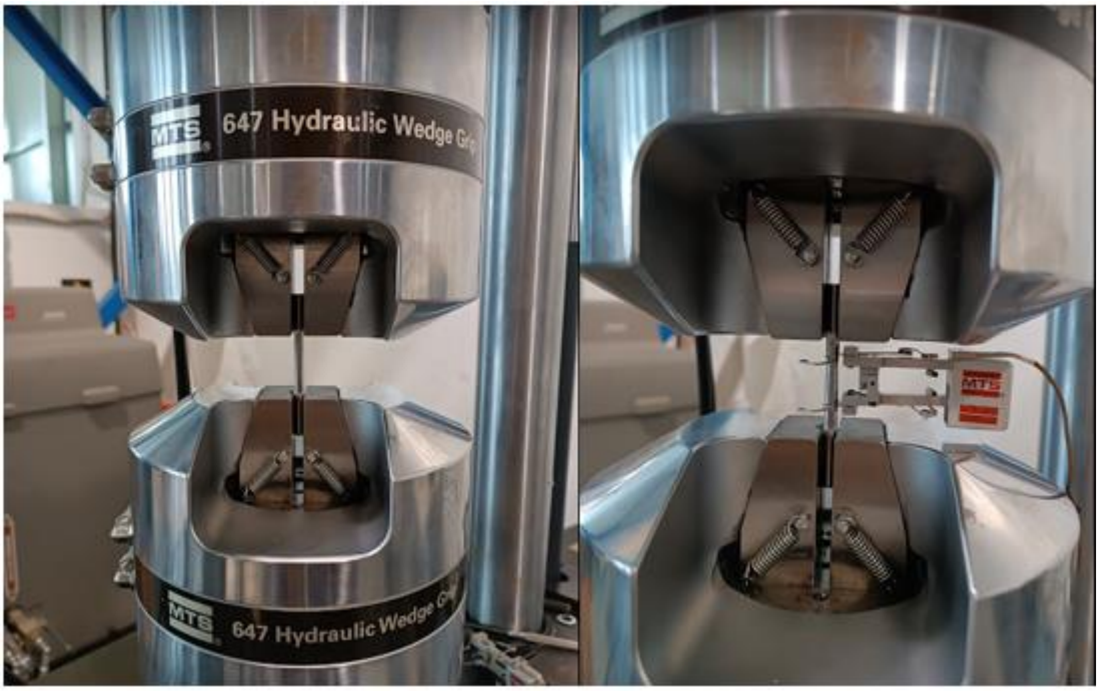
MTS
647 Hydraulic Wedge Grip
MTS
647 Hydraulic Wedge Grip
MTS

Figure 36: Tensile test and extensometer

8.1.1.1. 316L as built MBJ

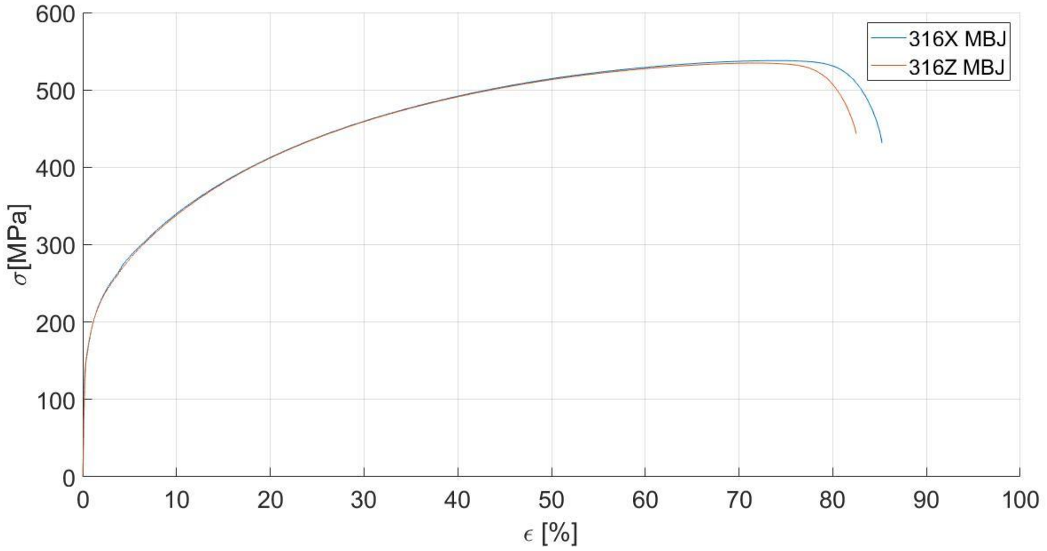

Figure 37: Tensile test 316 L AB in X and Z direction

316L	X Direction	MEDIA	DEV STD
	Sigma_yld [MPa]	169.64	3.20
	E [GPa]	162.06	5.58
	sigma_max [MPa]	537.17	2.00
	elongation [-]	85.3%	1%
	Number of samples	5	

316L	Z Direction	MEDIA	DEV STD
	Sigma_yld [MPa]	170.74	1.26
	E [GPa]	162.64	4.17
	sigma_max [MPa]	531.64	10.91
	elongation [-]	83.4%	3.2%
	Number of samples	5	

Here is tested austenitic stainless-steel 316L. Respecting other conditions, it presents the lowest tensile properties but the biggest elongation at breakage! For this reason, after the elastic region the velocity of deformation is progressively raised up to 3 mm/min. To decrease the test time.

In addiction the two directions are very similar also for mechanical properties and for elongation characteristics.

On the figure shown below its unambiguous to individuate that the material is totally ductile and see the plastic deformation on all of specimen.

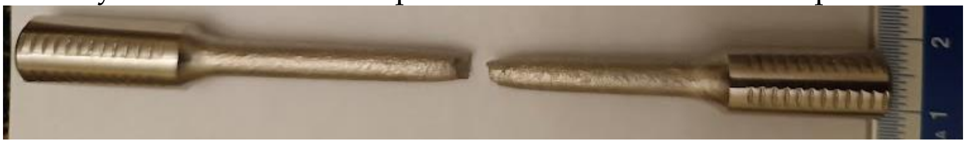

Figure 38: 316 L broken specimen

8.1.1.2. 316L Hip MBJ

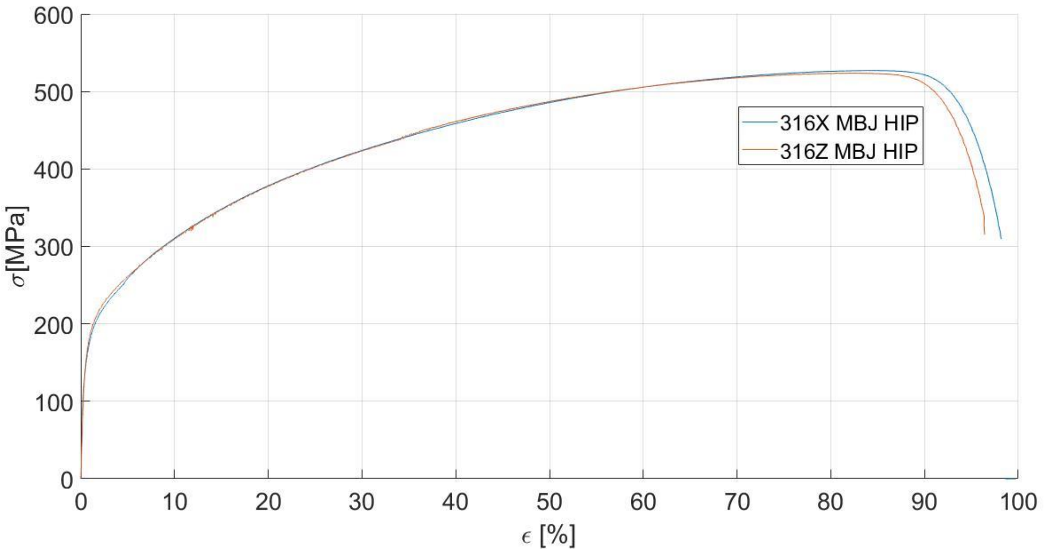

Figure 39: Tensile test 316 L HIP

316L	X Direction	MEDIA	DEV STD
	Sigma_yld [MPa]	159.19	3.72
	E [GPa]	138.34	13.61
	sigma_max [MPa]	523.24	3.02
	elongation [%]	99%	2%
	Number of samples	5	

316L	Z Direction	MEDIA	DEV STD
	Sigma_yld [MPa]	159.18	4.91
	E [GPa]	130.25	23.72
	sigma_max [MPa]	514.26	6.71
	elongation [%]	96%	1%
	Number of samples	5	

In Hipped condition the mechanical properties between X and Z become more similar. And make more isotropic the behavior of material. But inside this new class there is more dispersion between the curves.

As expected, the elongation increases significantly, but the stress admissible decreases a bit. These happen since the permanence of metal at high temperature for some hours permits the microstructure to change and make the grain bigger, this last condition decreases mechanical properties.

Another phenomenon that occurs is the shrinkage of porosity, that can be seen in density increasement (look at paragraph 8.2.)

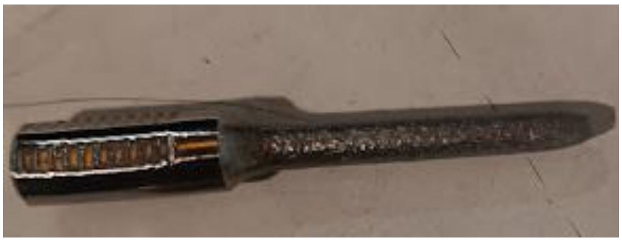

Figure 40: broken specimen

8.1.1.3. 17-4 PH As built MBJ

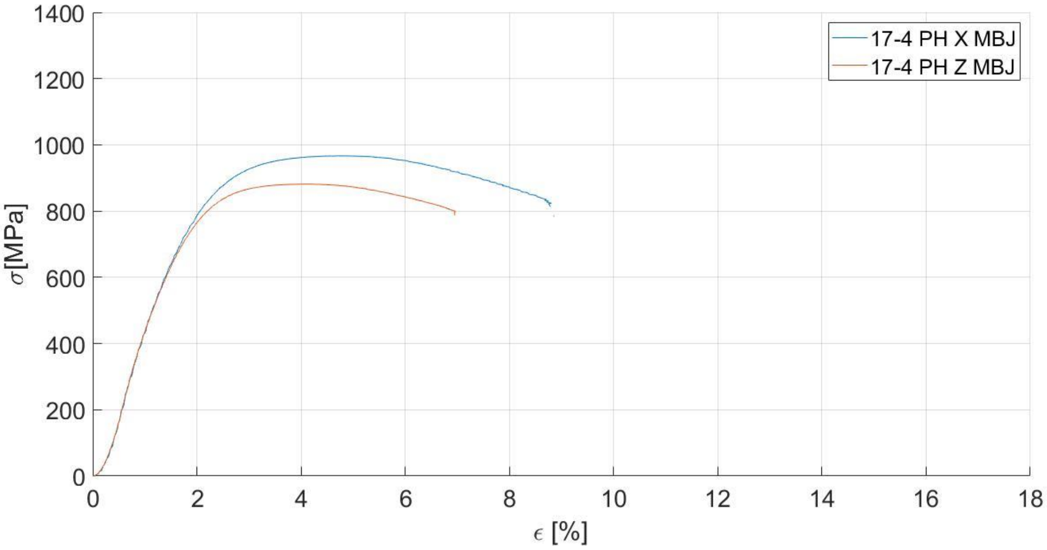

Figure 41: Tensile test of 17-4 PH

17-4 PH	X Direction	MEDIA	DEV STD
	Sigma_yld [MPa]	705.22	3.07
	E [GPa]	192.30	1.27
	sigma_max [MPa]	955.23	13.93
	elongation [%]	9.4%	1.2%
	Number of samples	5	

17-4 PH	Z Direction	MEDIA	DEV STD
	Sigma_yld [MPa]	670.47	5.51
	E [GPa]	194.08	0.99
	sigma_max [MPa]	890.55	5.75
	elongation [%]	8.3%	1.7%
	Number of samples	5	

The 17-4 PH is more performant respect to 316L but presents a higher dispersion of result between X and Z where X is the most performant.

In the figure shown below it is represented a specimen with a partial ductile behavior (looking at the cone formed by fracture)

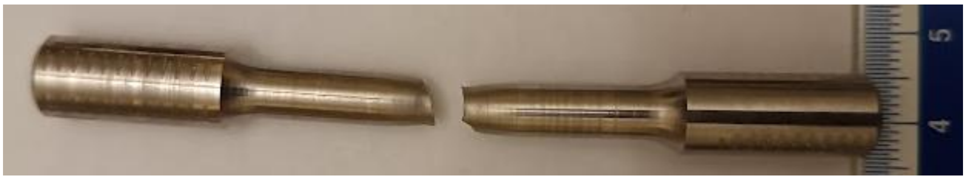

Figure 42: broken 17-4 PH specimen

8.1.1.4. 17-4 PH Hip MBJ

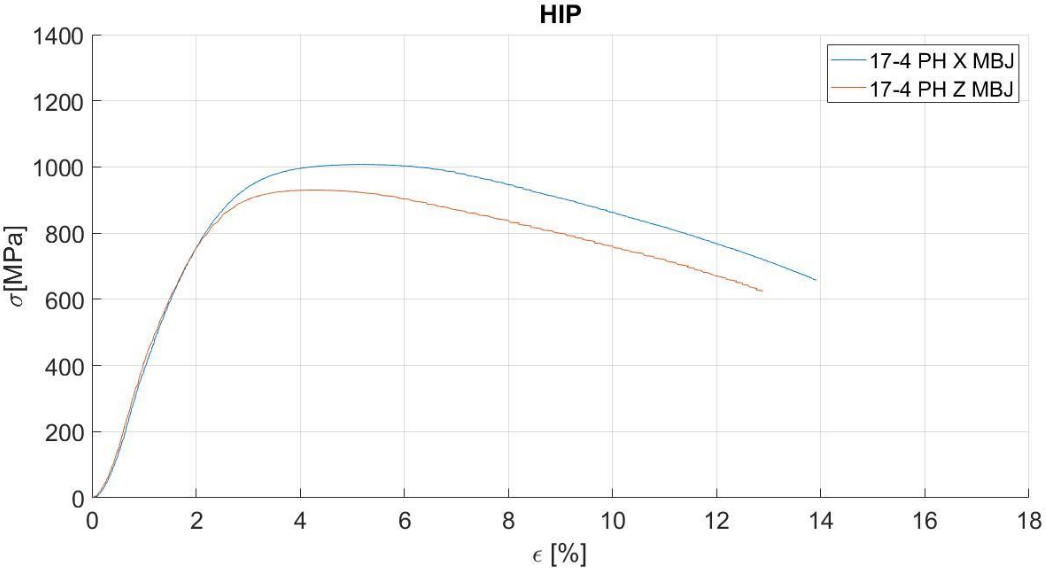

Figure 43: Tensile test in 17-4 PH HIP

17-4 PH	X Direction	MEDIA	DEV STD
	Sigma_yld [MPa]	731.81	1.97
	E [GPa]	197.29	1.34
	sigma_max [MPa]	1026.18	16.31
	elongation [%]	14%	0.5%
	Number of samples	5	

17-4 PH	Z Direction	MEDIA	DEV STD
	Sigma_yld [MPa]	712.23	10.31
	E [GPa]	195.54	2.57
	sigma_max [MPa]	933.84	8.16
	elongation [%]	13%	0.5%
	Number of samples	5	

Here the HIP treatment increases both mechanical properties and elongation.

The difference between X and Z direction remain markable, and also in this condition the better direction is X!

8.1.1.5. 17-4 PH H900 MBJ

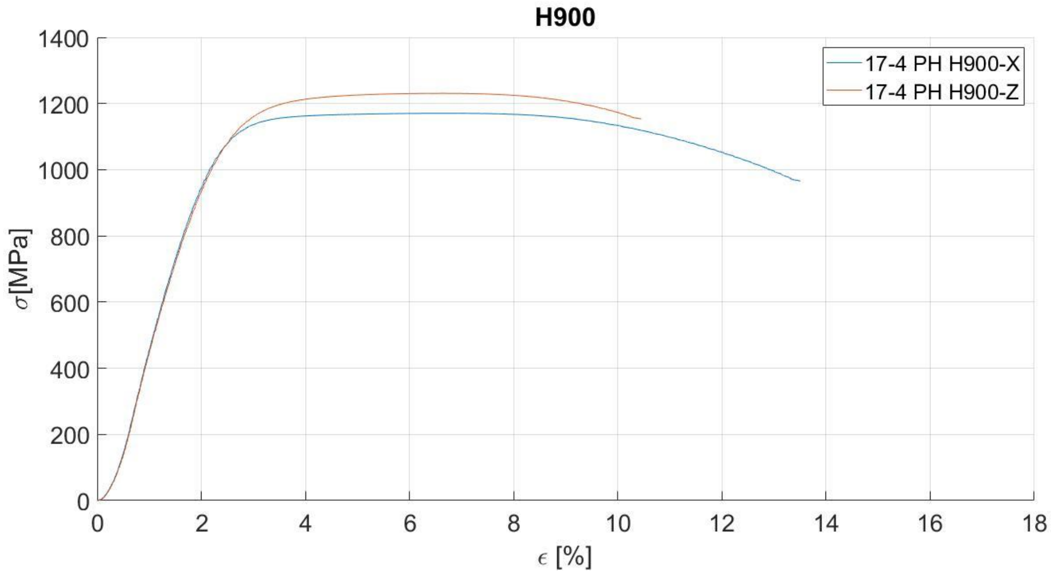

Figure 44: Tensile test 17-4 PH H900

17-4 PH	X Direction	MEDIA	DEV STD
	Sigma_yld [MPa]	1071.50	6.32
	E [GPa]	200.72	0.68
	sigma_max [MPa]	1178.22	13.45
	elongation [%]	14.7%	1.2%
	Number of samples	5	

17-4 PH	Z Direction	MEDIA	DEV STD
	Sigma_yld [MPa]	1050.37	9.38
	E [GPa]	201.00	1.42
	sigma_max [MPa]	1209.45	29.69
	elongation [%]	114%	1.8%
	Number of samples	5	

With Heat treatment the material became more brittle, also from fracture analysis it can be noticed.

The H900 is more performant condition, and also elongation increases. In addiction with heat treatment the difference between X and Z decreased noticeably. But now the most performing direction is Z!

In the figure below is shown the fragile behavior of this condition, in fact the fracture is perpendicular to the direction of the specimen.

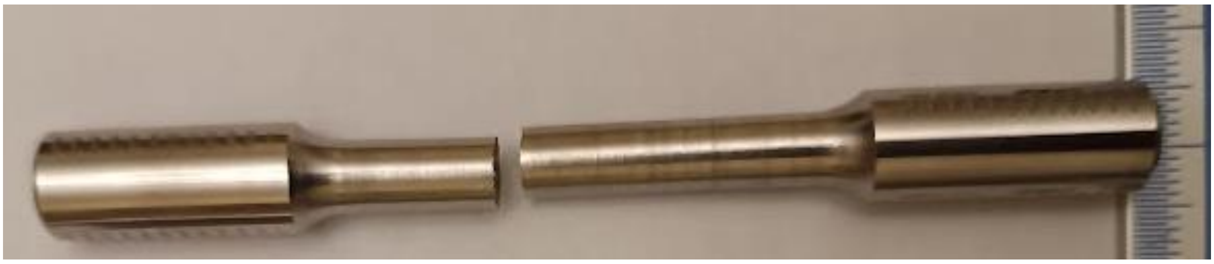

Figure 45: broken H900 specimen

8.1.1.6. 17-4 PH Hip + H900 MBJ

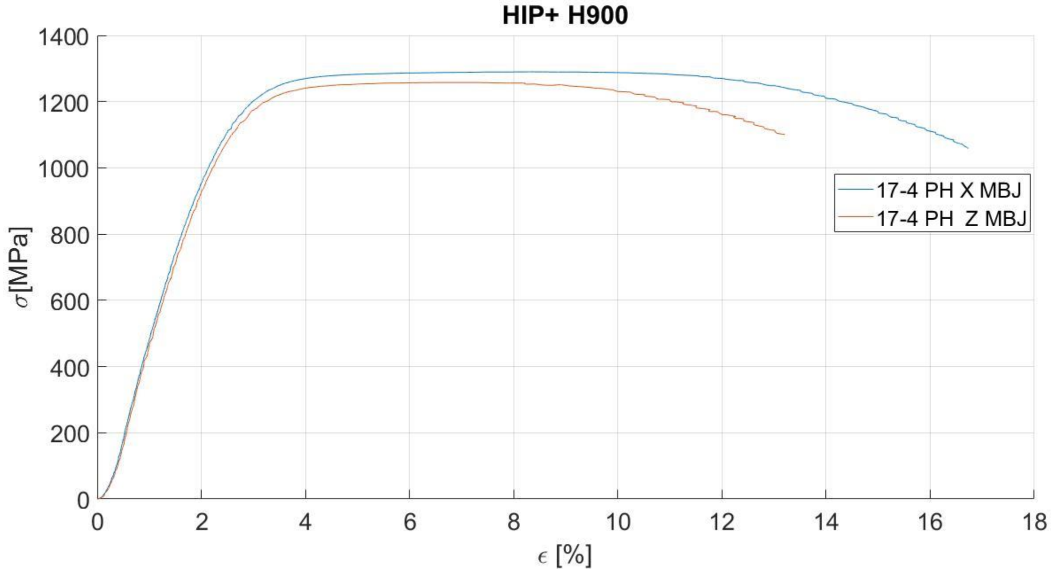

Figure 46: 17-4 PH MBJ HIP+H900

17-4 PH	X Direction	MEDIA	DEV STD
	Sigma_yld [MPa]	1167.10	4.08
	E [GPa]	186.28	1.54
	sigma_max [MPa]	1289.08	2.51
	Elongation [mm/mm]	16.36%	0.65%
	Number of samples	5	

17-4 PH	Z Direction	MEDIA	DEV STD
	Sigma_yld [MPa]	1148.76	5.58
	E [GPa]	184.69	0.37
	sigma_max [MPa]	1262.30	5.97
	Elongation [mm/mm]	12.55%	0.55%
	Number of samples	5	

Figure 47 :broken specimen 17-4 PH

This condition combines the benefit of two heat treatment, in particular the HIP treatment increase the capability to elongate (ductility) in fact it's possible to see that the broken section present a bigger necking.

In addiction with H900 the tensile properties increase a lot.

8.1.1.7. 17-4 PH LPBF As built

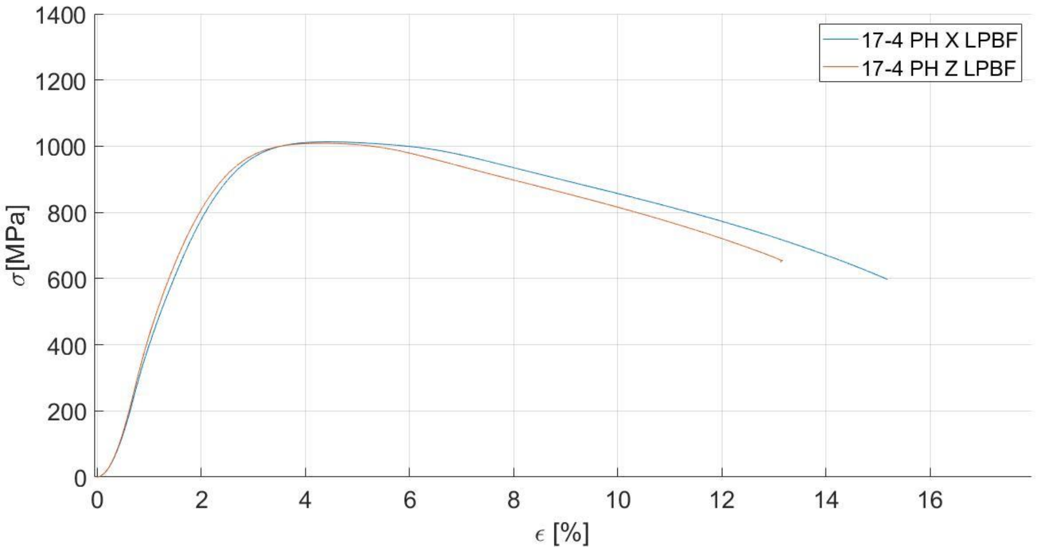

Figure 48 Tensile test 17-4 PH LPBF

17-4 PH	X Direction	MEDIA	DEV STD
LPBF	Sigma_yld [MPa]	807.66	5.75
	E [GPa]	194.67	1.36
	sigma_max [MPa]	1050.91	5.90
	Elongation [mm/mm]	14.3%	0.8%
	Number of samples	5	

17-4 PH	Z Direction	MEDIA	DEV STD
LPBF	Sigma_yld [MPa]	811.31	8.58
	E [GPa]	195.77	2.21
	sigma_max [MPa]	1055.02	7.13
	Elongation [mm/mm]	13.1%	0.4%
	Number of samples	5	

This condition is a tensile test from specimen given from EOS printed in a M290. As expected, Laser powder bed fusion has the best mechanical characteristic, both for σ and elongation, instead Young modulus remains constant respect to MBJ solution.

This better quality depends on the finer crystalline grain obtained thanks to fusion process that permits a precise point fusion and as consequence a very big cooling velocity.

8.1.1.8. 17-4 PH LPBF H900

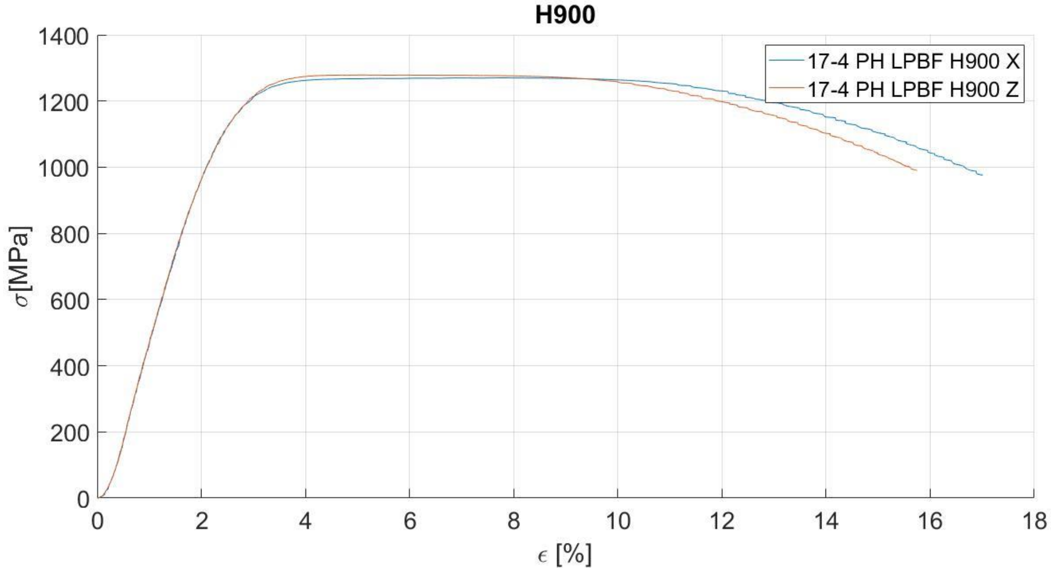

Figure 49: Tensile test 17-4 PH LPBF H900

17-4 PH	X Direction	MEDIA	DEV STD
	Sigma_yld [MPa]	1177.13	2.79
	E [GPa]	192.84	0.38
	sigma_max [MPa]	1271.24	0.45
	Elongation [mm/mm]	16.91%	0.24%
	Number of samples	5	

17-4 PH	Z Direction	MEDIA	DEV STD
	Sigma_yld [MPa]	1176.99	18.06
	E [GPa]	191.21	3.19
	sigma_max [MPa]	1279.32	5.11
	Elongation [mm/mm]	15.03%	1.21%
	Number of samples	5	

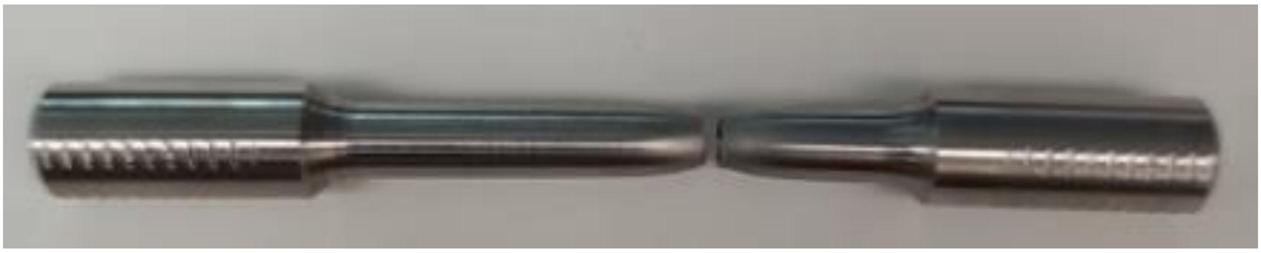

Figure 50: Broken specimen of 17-4 PH H900

8.1.2. Fatigue test

For the studied campaign is used an MTS 647 Series.

The fatigue tests are organized in this way: first of all, each specimen, as for tensile test, are marked in order to be recognized (number of job, batch powder, parameter used for job (layer thickness, saturation level, velocity of roller, humidity parameter)) for MBJ. Since LPBF Samples came from external company they was labelled in order to identified position on building plate and if it was in as built condition or heat treated.

It's chosen to test and compare two condition of 17-4 PH, more interesting respect to 316L for structural behavior, in H900 condition, since from Charpy test result [21] that is the most critical respect to energy absorption, that is correlated to fracture mechanism of fatigue.

Before starting the test, the parameters are setting:

- Frequency of oscillation: 20 Hz
- Run out: 1000000 cycles
- R= σ _min/ σ _max: 0.05
- Sigma level at which test: (90%,85%,80%,75%,70%,65%,60%) σ_{yld}
- Stair case:
  - 5 specimens
  - $\Delta\sigma = 20$ MPa
  - $\sigma_0 = 60\% \ \sigma_{yld}$

Then to analyze the result it is chosen to compare different method: ML (Maximum Likelihood) vs LMS (Least Means Square)

LMS is the abbreviation of Least mean square, this is the simplest method to evaluate statistical parameter from fatigue test, but it has some problems:

- Run out specimens have a diametrical opposite meaning respect to other specimens, but in this method, they are treated in some way causing an error!
- With LMS each stress level has same meaning, but in reality, for each stress level the data are disperse as gaussian, so a data at 3% percentile has same weight of a 50%
- LMS gives same accuracy level on all of measuring range, instead ML have a better confidence level around mean data that are tested

Also, the staircase method is based on ML method, since it is the best way to consider the physics of statistic of this test.

Fatigue Test MBJ H900

Stress Max. (MPa)	%	Cycles to Fail (N_f)
630	60	1000000
840	80	112706
735	70	119868
945	90	14911
735	70	154046
840	80	31752
945	90	36502
735	70	185642
840	80	39236
945	90	30046
893	85	28900
788	75	118976
683	65	391745
893	85	55702
788	75	51822
683	65	138532
650	61.90	1000000
670	63.8	531100

650	61.9	283846
630	60.0	481241

Here it is all the data collected in table where are analyzed at % respect to σ_{yld} :

- 3 stress level (90%, 80%,70%) σ yielding with 3 measures
- 3 stress level (85%,75%,65%) σ yielding with 2 measures
- 5 stress level for staircase method

8.1.2.1. Least Mean Square

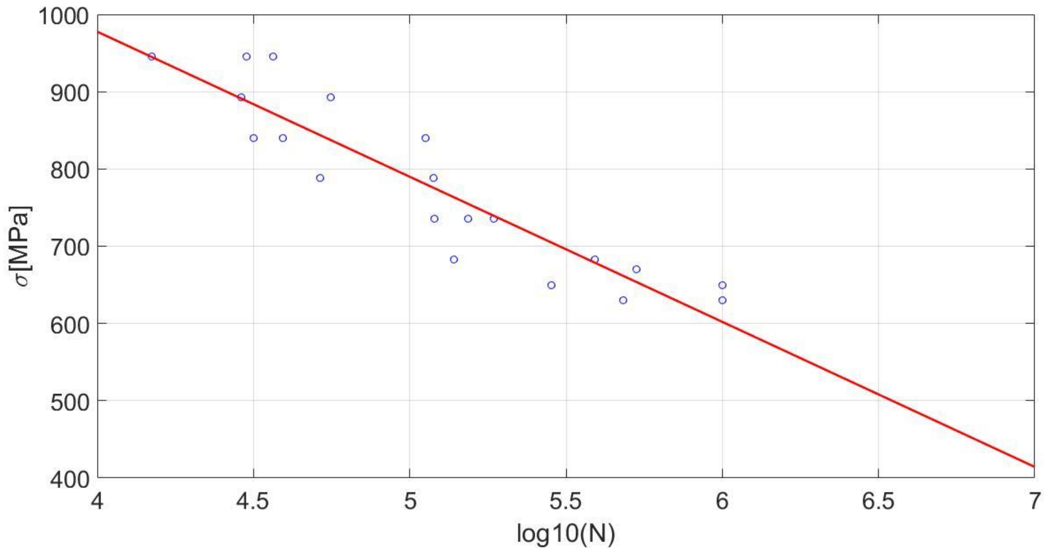

Figure 51: LMS fatigue approximation

$$\sigma = -187.7528 \times \log_{10}(N) + 1728.5$$

[22]

As seen before this method is fast and simple, useful to have a general idea of how the data are dispersed on the diagram but does not consider the statistical distribution of process.

8.1.2.2. Maximum Likelihood

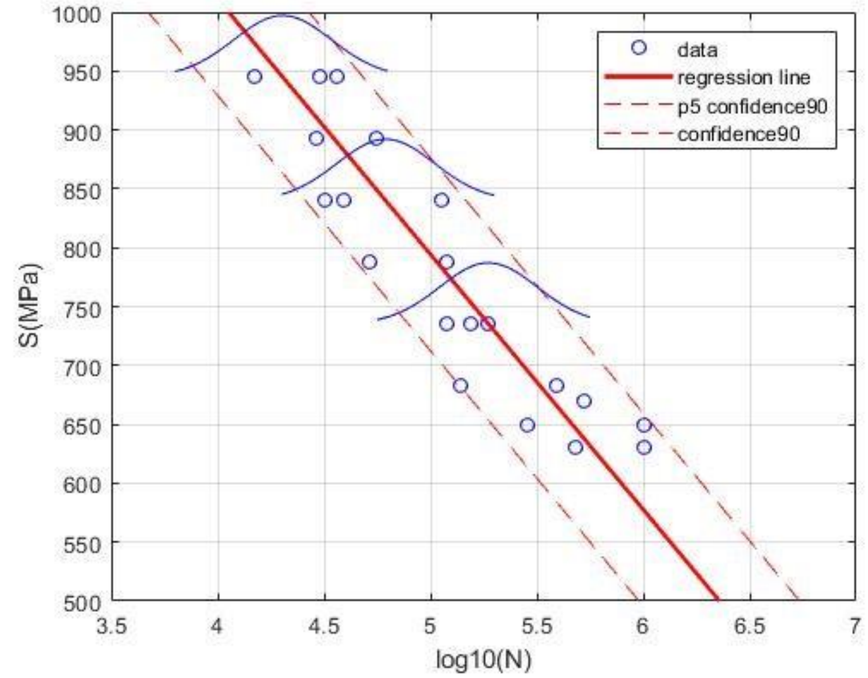

Figure 52: ML fatigue approximation for MBJ H900 samples

$$\sigma = -216.77 \times \log_{10} N + 1878.3 \quad [20]$$

$$\sigma_{5p} = -216.77 \times \log_{10} N + 1796.42 \quad [21]$$

On the figure is represented the trend of Wohler diagram using a ML method:

With this method, from input data and knowing the statistical distribution at which data belong, from literature it is seen that gaussian dispersion is the best approximation for this problem, it returns the value of parameter that identified distribution (in this case mean μ and std σ).

The Wohler curve, for its definition is the value at which it is a probability of 50% that specimen will break, in other worlds is the representation of mean value of each gaussian at different stress level.

Analyzing the curve, and suppose that std is equal for each level (reasonable approximation) it possible to obtain different curve at different probability of rupture:

Considering 5% percentile of the curve: it represents the specimen with a probability of rupture of 5%.

Considering 95% percentile of the curve: it represents the specimen with a probability of rupture of 95%.

Changing confidence bound it's possible to evaluate different probability of breakage.

In particular it's possible to obtain the desire curve translating the line in x-direction of a value:

$$k = K_\gamma \times \sigma\text{-}216.77 \qquad [22]$$

Where K_γ = norminv(1-p), and (p=perentile)

that is the function of normalized gaussian (μ=0 and std=1) that from a level of percentile returns the x-value of cdf .

And σ is the standard deviation of data population.

$$Yp = -216.77 \times \left(\log 1\,0(x) - k(p)\right) + 1878.3 \qquad [23]$$

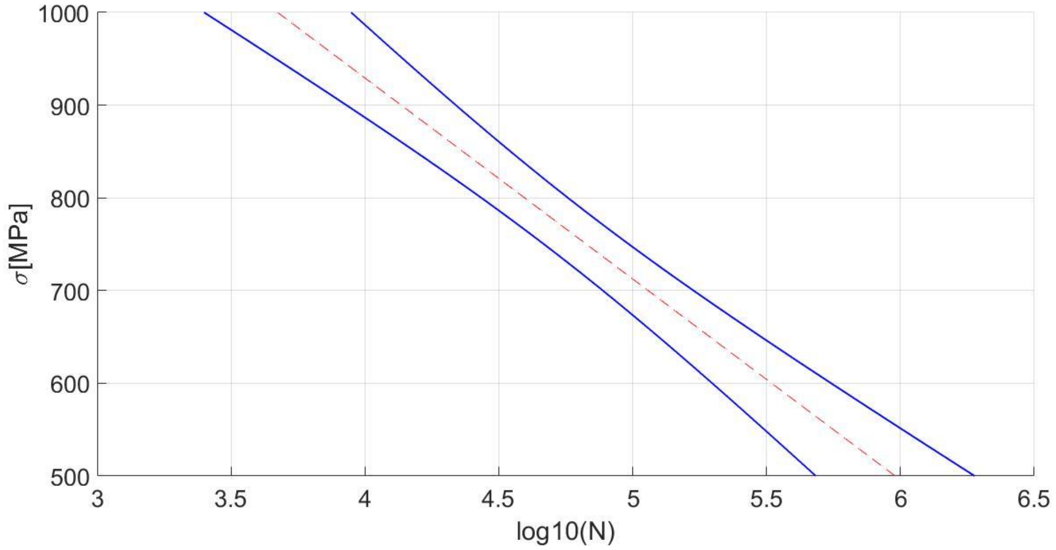

Figure 53 confidence bound of 95% respect to 5% percentile

From a statistical point of view when it’s needed to estimate a parameter it is useful to add a confidence bound, intended as the reliability that real value of N lays in the estimated interval in 95% of cases.

Clarifying: confidence bound is not referred to a probability, but at accuracy of estimated method.

Since the method is built from the mean value of sigma, here the confidence bound is more precise!

8.1.2.3. ML vs LMS

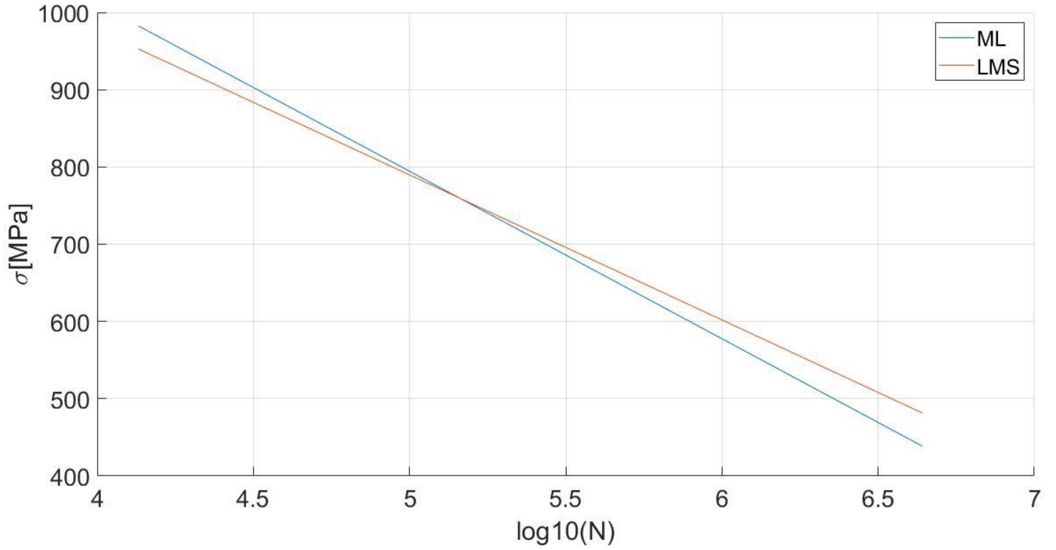

Figure 54: comparison between interpolated data ML vs LMS

Looking at comparison between two method is easy to see that ML is more conservative below the mean of stress level tested, and less conservative at high stress level at lower Number of cycles, this means that it is more safety at higher number of cycles.

In addition, with ML it is possible to make statistical considerations.

8.1.2.4. Staircase method

STAIR CASE METHOD											
STRESS LEVEL	MAX SIGMA	ID SIMPLE					RESULT				
i		1	2	3	4	5	X	O	N	A (n*i)	B (n*i^2)
2	670			X			1	0	0	0	0
1	650		O		X		1	1	1	1	1
0	630	O				X	1	1	1	0	0
						Σ n	3	2	2	1	1

A=1, B=1; N=2.

$$\sigma_{D_{50\%}} = \sigma_0 + d\left(\frac{A}{N} \pm 0,5\right) = 630\ MPa$$

[24]

$$s = 1,62d\left(\frac{(NB - A^2)}{N^2} + 0,029\right) = 9.04\ MPa$$

[25]

Staircase Method is done with 5 specimen and 3 level of stress.

Following the formulas proposed by Method (Dixon and Mood) the result is that fatigue limit is 630 MPa and its standard deviation is 9.04 MPa. This method is powerful because it can condensate a statistical dispersion of data into a single variable.

8.1.2.5. LPBF H900 Z direction

In this thesis the purpose is to compare same material (17-4 PH) and same heat treatment (H900) done with same thermal curve in two different laboratories (DAER and Tav)

Before starting the test, the parameters are setting:

- Frequency of oscillation: 20 Hz
- Run out: 1000000 cycles
- R= σ _min/ σ _max: 0.05
- Sigma level at which test: (90%,80%,70%,60%) σ_{yld}
- $\sigma_{yld} =$ 1177
- Total number of samples: 10

This last number was fixed by time problem, from a statistical point of view isn't the best choice but in the future more studies will be done with this configuration.

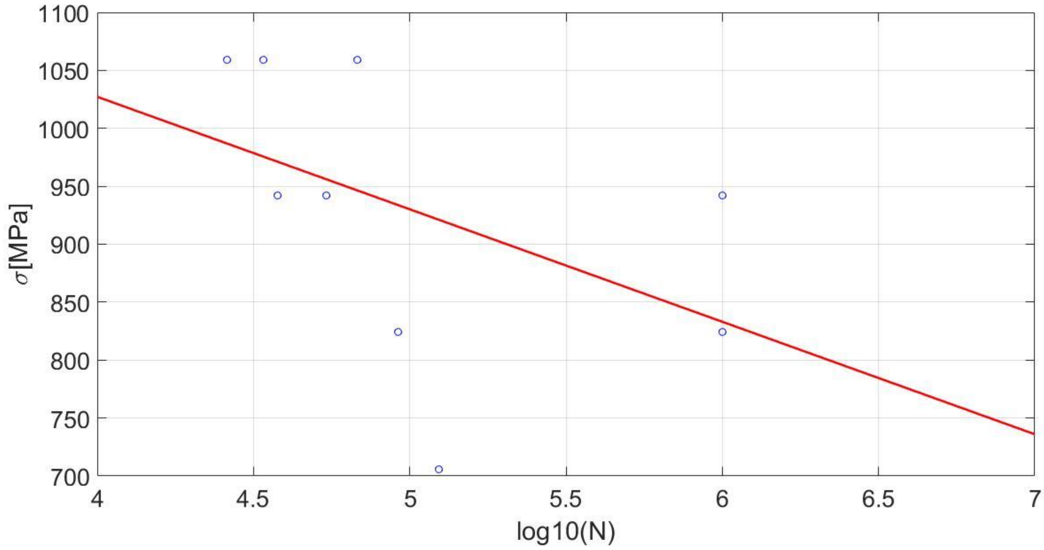

Figure 55: Fatigue life of 17-4 PH H900 LPBF with LMS Method

In the figure 55 is possible to see the LMS approximation of the data collected , following is shown the equation that represent the line :

$$\sigma = -97.07 \times \log_{10}(N) + 1415.48 \qquad [26]$$

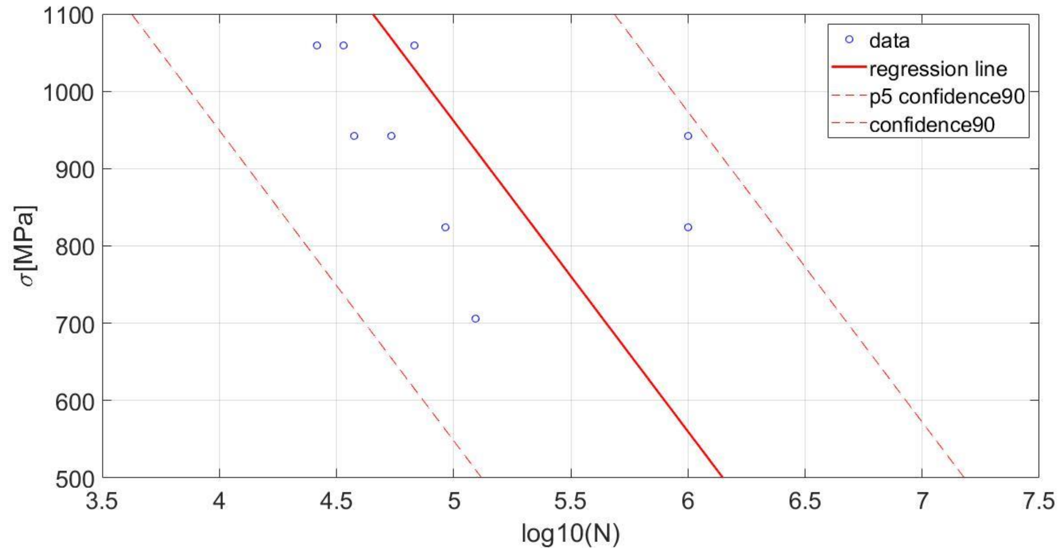

Figure 56: Fatigue life and 5% percentile of 17-4 PH H900 LPBF

In the figure 56 is represented the Wohler diagram with 5% percentile and 95% percentile , as it's possible to see the data are very disperse

$$\sigma = -401.4 \times \log_{10} N + 2968.7 \quad [27]$$

$$\sigma_{5p} = -401.4 \times \log_{10} N + 2555.3 \quad [28]$$

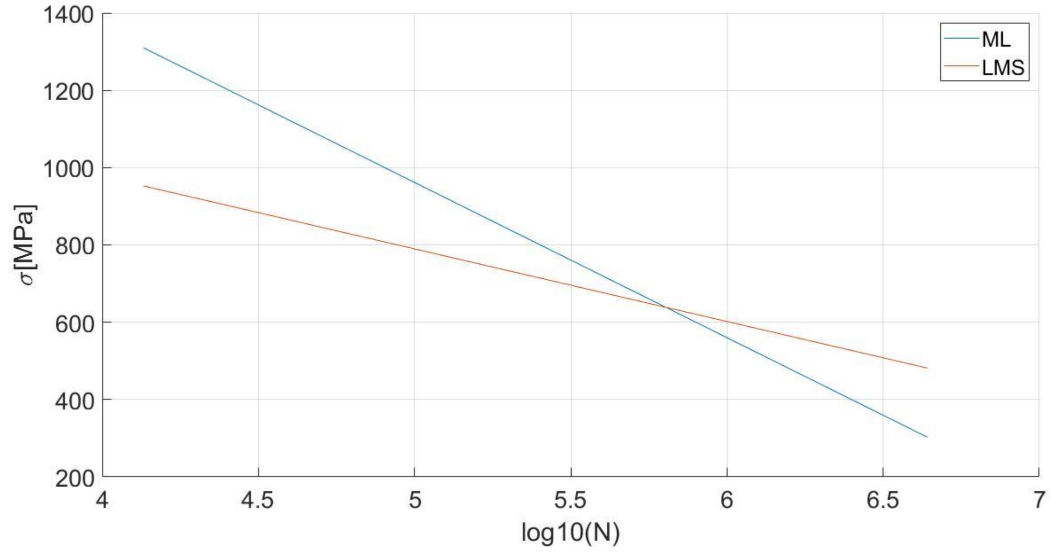

Figure 57: comparison between ML and LMS of 17-4 PH H900 LPBF

Looking figure 56 is possible to see that ML and LMS method are relatively different, this is due to the high dispersion of data.

As in MBJ the ML is more conservative at high number of cycles.

8.2. Density measurements

The density measures are done with a Gibertini Europe 500, a balance with a precision of 0.001 g.

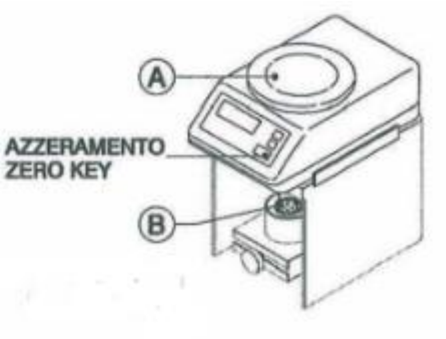

Figure 58: balance used in density measurements

Measures are done for 4 different configurations of 17-4 PH and 2 condition of 316L.

Considering 17-4 PH the measures are done on cubes of 20x20 mm for

- MBJ as built condition
- MBJ H900
- MBJ HIP
- LPBF as built

Considering 316L:

- MBJ as built
- MBJ HIP

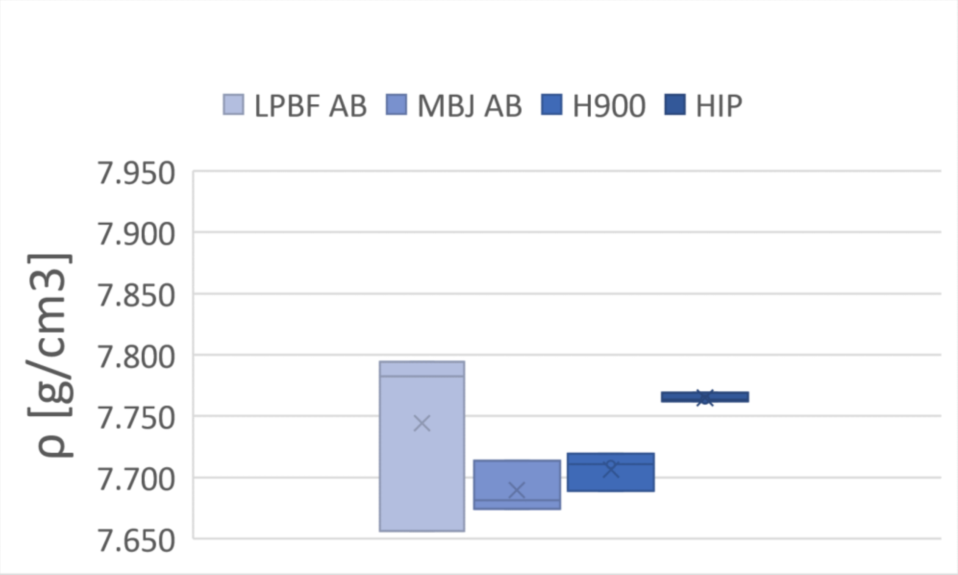

Figure 59: density measurement for 17-4 PH

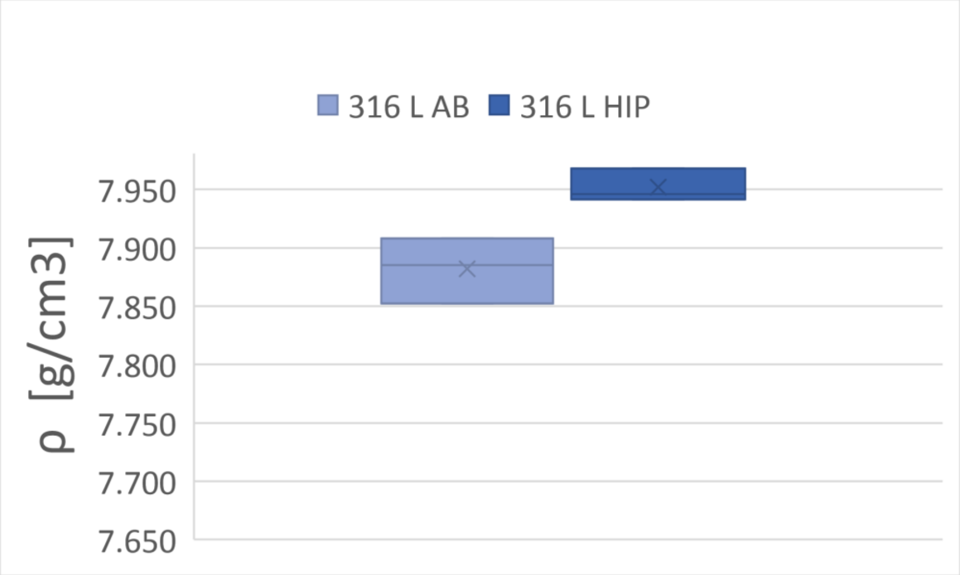

Figure 60: density measurement for 316L

As it was expected HIP treatment has the capability to shrink close porosities, so it's easy to understand that the density increase! This has effect also on mechanical properties,

On the other hand, H900 treatment seems not to have effect on density but only on mechanical properties.

8.3. Porosity

Porosity is a critical issue for each AM component since its own production process has this typology of defects. Each company, depending on what is level of criticality is, has some requirements to respect.

The main aspect is:

- Scanning each section of surface there is a size of pore that can't be bigger than a certain level.
- Analyzing determined part of section, at least 4 for have a statistical meaning, the porosity level, defined as Area of pores divided total area of picture, need to be under certain level

In addition to avoid taking some edges effect the selected part needs to have a distance of at least 1mm from edge.

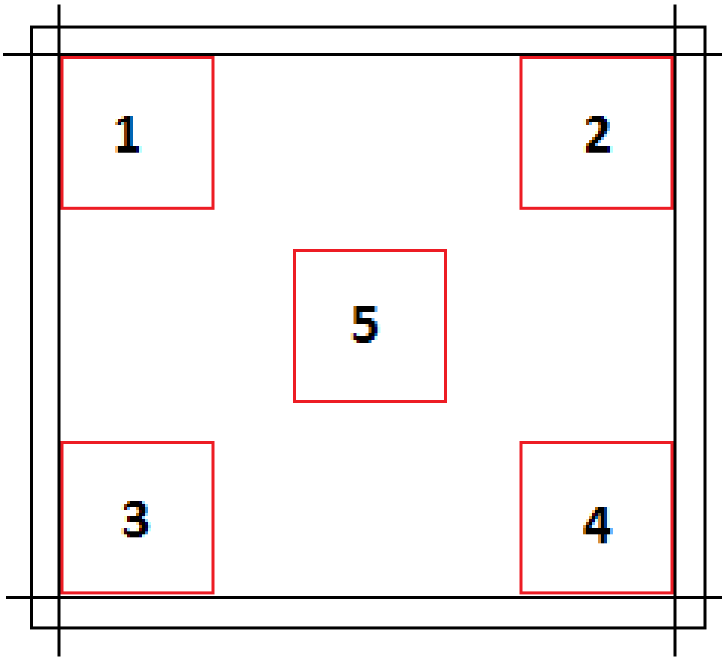

Figure 61: Sampled Areas

8.3.1. Samples preparation

The preparation of metallographic specimen is standardized following ASTM E3.

The cubes are a 20x20x20 mm for MBJ and 15x15 for LPBF.

The analyzed configuration are:

	MBJ AB	LPBF AB	MBJ HIP	MBJ H900
316L	X	-	X	-
17-4 PH	X	X	X	X

They are cutting with a metallographic cutting machine, a machine that utilizes a circular saw and a refrigerator liquid in order to not change the microstructure level.

It has been chosen as cutting direction z

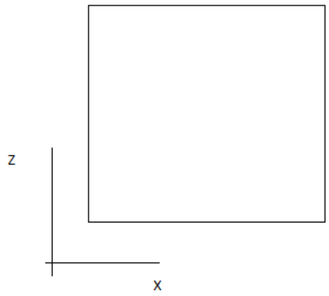

Figure 62: sample orientation in microscope

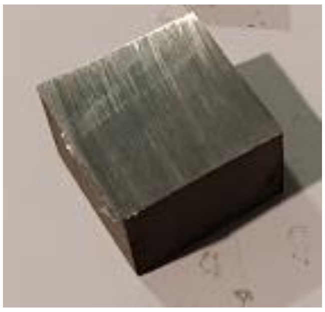

Figure 63: Cutted cube

Then they are lapped with different sandpaper with different grains until they are polished in a very precise way.

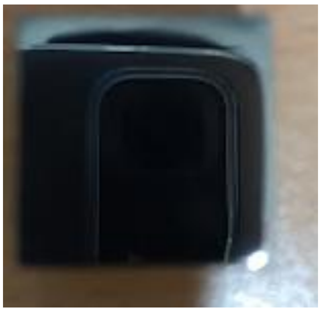

Figure 64: lapped cube

Then using SEM HitachiTM3000 at 60x magnification and using ImageProPlus as post-processing software it's vas easy to see pores and their relative weight on the entire section (null).

TM3000
HITACHI

Figure 65: SEM HitachiTM3000

Shown below some samples in order to understand how the software works.

- Choosing an imagine to analyze.
- Then modify contrast and brightness in order to have a white background and black porosity
- The software counts the number and relative dimension of area of pores
- In the end summing all relative area of pores it was ready to have the integral porosity on the whole area

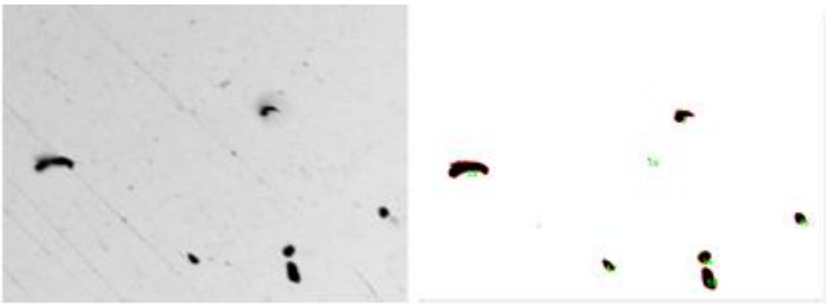

17-4 PH HIP MBJ Rho=99.081% magnification 150x

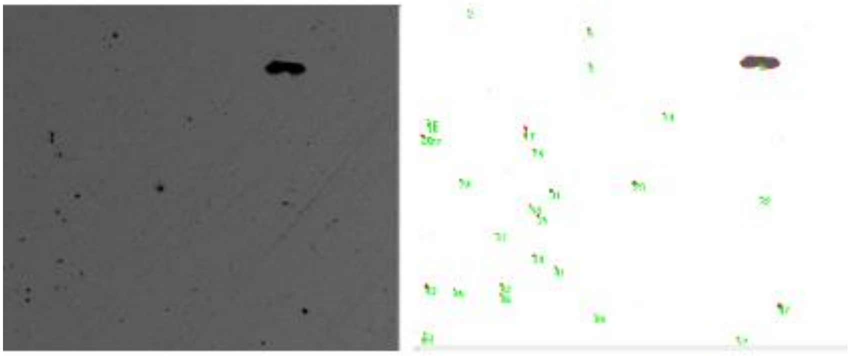

316L MBJ Rho=99.66% magnification 150x

Figure 66: example of sampled section

The following measure are the arithmetic mean of 5 measurements for each configuration:

POROSITY MEASUREMENT	MEAN
316L AB MBJ	99.851%
316L HIP MBJ	99.953%
17-4PH AB MBJ	99.923%
17-4 PH H900 MBJ	99.897%
17-4 PH HIP MBJ	99.968%
17-4 PH PBLF	99.991%

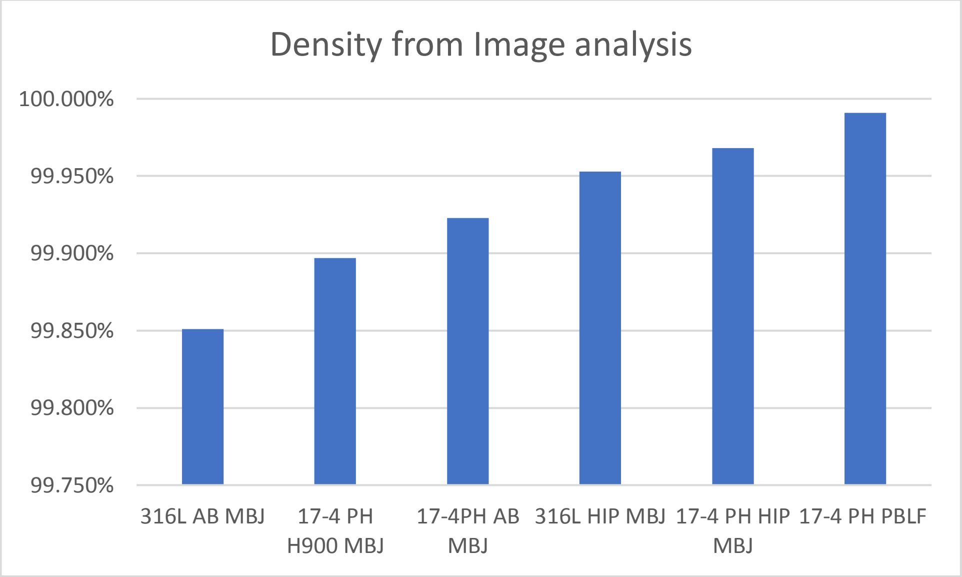

Figure 67: density from SEM imagins

HIP treatment reduces porosity since that density found with image analysis is noticeably increased.

8.4. Fracture analysis

Analyzing fracture after the specimens broke it can be useful to investigate how type the fracture is:

For tensile test the main group in which the fracture can be divided is fragile and ductile.

To analyze these types of fracture it’s been used a SEM. Following there is a brief explanation of how it works.

8.4.1. SEM

The main principle behind SEM is that electrons are fired at the surface of a specimen. These electrons will interact with the atoms on the surface, and information can be gathered by recording the various signals that the excited atoms emit. The electrons fired are called primary electrons and are fired from the electron gun. The electrons are accelerated through a condenser to give them high energy. The primary electron beam is run across the interest area in a raster scan method. The samples must be clean and must be able to withstand the vacuum atmosphere. Another important note is that the specimen must be electrically conductive and grounded to dissipate the charge build up.

Secondary electrons SE

Secondary electrons are electrons that are knocked of the specimen atoms, they are relatively low in energy. Because of their low energy, they have little penetrating capacity under the surface. The electron detector will therefore only detect secondary electrons that emanate in close proximity to the initial electron beam, resulting in a high-resolution image. This gives the capability of mapping the topology of uneven surfaces, for example fracture surfaces.

Backscatter electron BSE

Backscatter electrons are electrons that are scattered elastically, meaning that they are the primary electrons, but their trajectories have been altered after interacting with atoms in the sample. These electrons have higher energy than that of SE, thus they can propagate deeper through the material. This means that the resolution will be poorer when picking up BSE. The signal of BSE on a given point is related to the atomic number of the atom, higher Z numbers give a higher probability of BSE. Heavier elements will appear brighter compared to surrounding lighter atoms. Lighter elements will appear darker. BSE can display local variations in atomic numbers.

Energy dispersive spectroscopy EDS

The primary electrons can interact with a surface atom in such a way that an electron is knocked off, typically from the k shell or L shell. The atom is unstable in this state, and an electron from a higher shell will fall down to replace the vacancy. This results in a discharge of an x-ray photons, the energy of the photons is characteristic to the atoms they emanate from. EDS gives the capability of qualitative composition analysis of pinpointed areas on the specimen surface.

8.4.2. Fractography

Information about a materials property can be ascertained by analyzing its fractured surface.[22] Observations can be gathered in a wide range of ways, from visually observing directly with eyesight, to electron microscopy. This thesis is mainly focused on fractography by way of SEM.

SEM allows for studying the fine topology of the fracture surface. Generally, the observable features on the surface can be regarded as evidence of ductile or brittle fracture. However, this can be misleading as these features often appear in combination.

Dimples

The presence of dimples is an indicator of ductile fracture. When a material is subjected to a tensile load the material starts to stretch. Small micro voids start to nucleate from imperfections, like inclusion. The voids grow in size, and when they coalesce, they have effectively separated the material allowing the crack to propagate. The resulting surface left behind has the characteristic half spheres, this is referred to as dimples. The mechanism of micro voids coalescing to become a crack is referred to as micro void coalescence. The dimples will sometimes contain an inclusion, this is the point of nucleation.

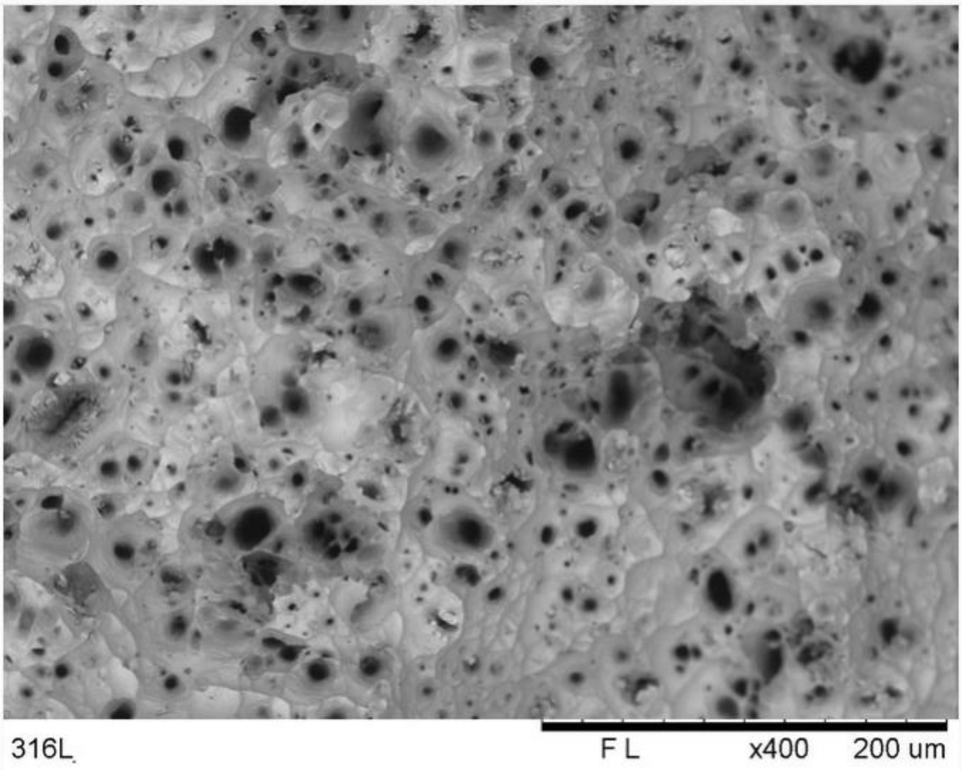

Figure 68: broken specimen after tensile test

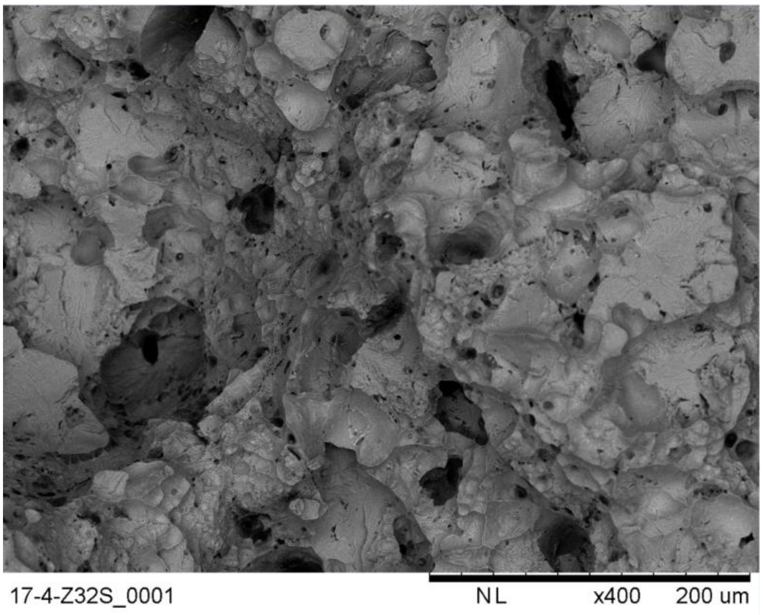

Figure 69: dimples and trans granular fracture

Intergranular fracture

Fracture displaying granular features, the fracture has followed the grain boundaries is referred to as an intergranular fracture. Its presence indicates a brittle fracture.

Possible reasons for intergranular fracture are the weakening of the grain boundaries. This can happen through for example, hydrogen embrittlement or stress corrosion cracking, these mechanisms attack the high energy grain boundaries.

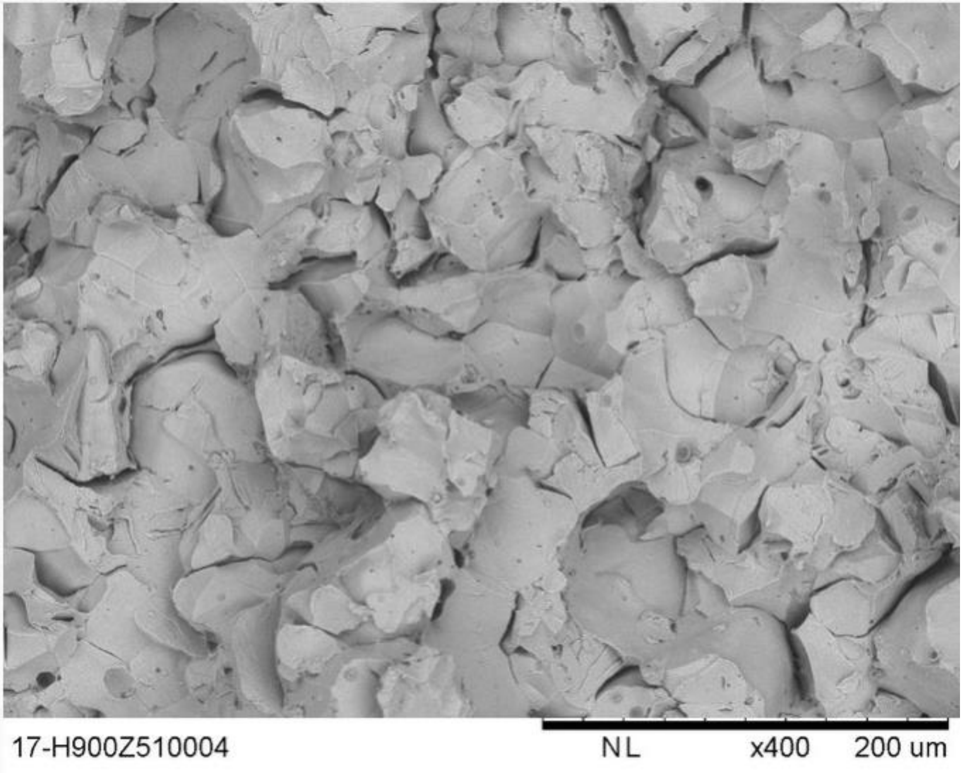

Figure 70: Intergranular fracture without dimples

Transgranular fracture

The fracture occurs along the crystallographic planes instead of following around the grain. The fracture mode is therefore often referred to as a cleavage fracture. The direction of crack propagation will often not coincide with the crystallographic plane inside the grain, so the crack must shift between parallel layers to maintain the direction of the crack travel. This is the explanation behind the river phenomena that is typically associated with cleavage fracture. The direction of crack propagation can also be ascertained by studying the rivers. Flowing from the branched end to the thicker end. Another feature that can be found on a cleavage face is a so-called tongue. Tongues appear as thin layers on the cleavage face, they are the result from when the cleavage start to follow a twin grain orientation for a short while before falling back to the original plane.

A material that does not have clear cleavage plane, like that of a martensitic structure, is said to display quasi cleavage fracture faces [21]. The surface can consist of smaller fragments of quasi cleavage faces, initiated by surface defects in the material.

9 Conclusion and future developments

The main aim of this thesis were:

- comparison between the behaviour of stainless steel 17-4 PH produced with different AM technologies (MBJ and LPBF).
- See the effect of heat treatment of HIP and H900

Globally, as it was expected the 17-4 PH produced by LPBF is more performant respect to MBJ, but the result are comparable.

The **HIP** effect is :

- globally increases the density of raw material, that means it close the internal porosity, making the material more resistant to cycles load. In addiction for this reason the material becomes more ductile, and the elongation at fracture increases.
- reduces the difference between X and Z direction making the material more isotropic.
- On the other hand it not have a great impact on mechanical properties.

The **H900** instead increase a lot the mechanical properties of material and also the elongation at fracture!

For MBJ the **HIP + H900** treatment increase much more the mechanical properties (best condition for maximum stress condition). This can be expected since the HIP treatment improve the quality of metal matrix and H900 can work in a better way.

During this characterization campaign

- **40 fatigue samples** have been tested printed in Z direction produced half in MBJ and half in LPBF.
- A total of **80 tensile samples** have been test printed in different orientation and with different technologies (see paragraph 8.1.1)

9.1. Porosity

Porosity of material can be analyzed from two type of test:

- Image Analysis
- Density measurement

The tests done in this work are limited in number and for more accuracy of result it will need a more series of tests but from these measures some consideration can be made:

From the comparison between the two measures, it has been seen that comparing MBJ

- 316L relative density is bigger respect to 17-4 PH

Comparing 17-4 PH made by MBJ and LPBF

- As expected MBJ relative density is smaller respect to LPBF but with HIP treatment the two are comparable

The porosity is an important characteristic that can infect many properties of material:

- The fatigue behavior can be influenced by porosity, since the lack of material correspond to less resistant surface in addiction from a internal pores a crack can start, reducing the normal fatigue life of material
- The corrosion resistance is also influenced by porosity since an external pores can lead inside the material some oxides or acid particle that inside pores can easily corrode the material

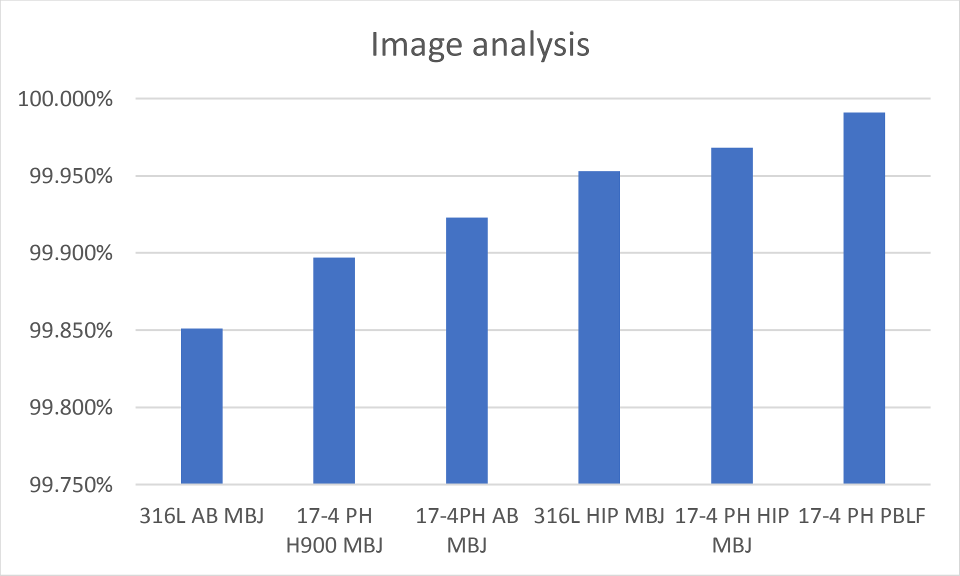

Figure 71: density comparison among different condition

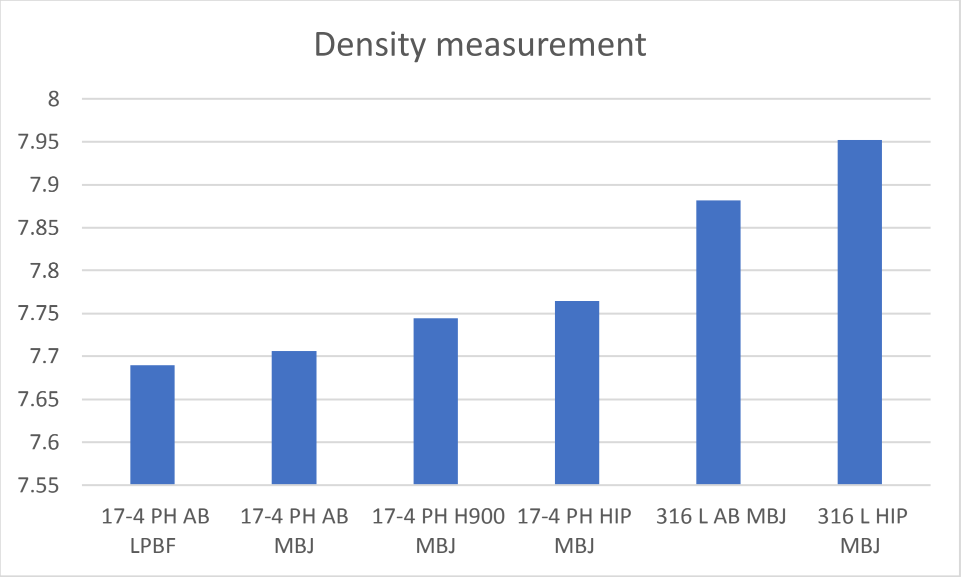

Figure 72: density comparison among different condition

Looking at figure 72 is possible to see the absolute density of all condition taken into account, as general trend can be observed that :

- HIP increase the absolute density in each consideration
- 316 L has bigger density respect t 17-4 PH (as expected from each composition)

9.2. Tensile test

In this work a lot of configurations have been tested, reassuming:

- 316L properties remains almost constant after HIP (a small decrease of E and σ_{yld} can be observed but is comparable with std deviation)
- 17-4 PH from LPBF have better properties respect to MBJ in as built condition
- 17-4 PH from MBJ and LPBF react well to heat treatment

Some consideration can be done:

316L isn't good as structural material since it's plastic and its yielding point is very low. Its best quality in fact from literature [25] is its corrosion resistance.

9.3. Fatigue test

In this work the main aim is to evaluate the fatigue behavior of MBJ technology, comparing it with behavoir of LPBF with same material and same heat treatment.

From result (see paragraph 8.1.2) it can be observed that the material respond in a better way (more high load level) but in a more random way.

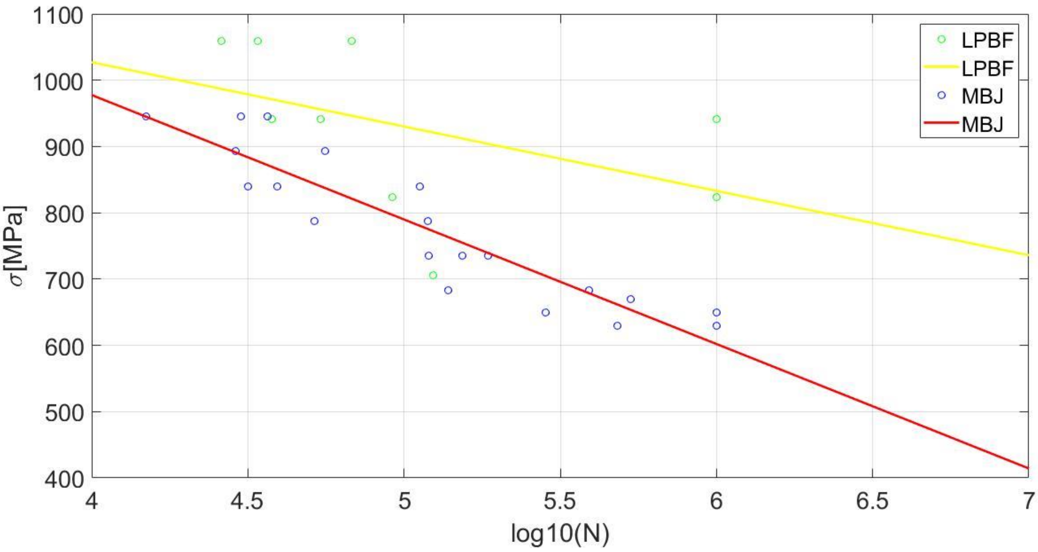

Figure 73: comparison fatigue data between LPBF and MBJ of 17-4 PH

Probably its due to :

- At higher load the material responds in a more random way because it has difficulties to share the stress locally
- For LPBF technology has less pores but their dimension is bigger [30] and so a fracture can start easier respect to MBJ

9.4. Future developement

MBJ is a very interesting technology with high potential, but since it's a new technology it requires a lot of test and studies to improve the quality of the result and find the right field of application. Some studies have been done comparing the MIM technologies [26], that have the same family of process of manufacturing of MBJ but a lot of work must be done.

Some studies of LCA have been starting to understand the real environment impact of this new technologies.

One of the problems of MBJ is the porosity of material and investigate how it is distributed inside the volume, how change respect to position in the building plate is a very interesting part that needs to be investigated.

Another aspect to be investigate is to verify that HIP treatment increases the corrosion properties of material and improve the surface quality.

Taking in account 316 L, the worst condition looking at mechanical properties, it will be necessary to find some heat treatment to improve its resistance.

And concluding with fatigue analysis a lot of test must be done, this work contains one of the first campaign of data on 17-4 PH made by MBJ but since the fatigue is very sensitive to each configuration and for time-problem in this work the run-out is fixed to 10^6 cycles more test is required to find the real behavior to infinite fatigue life of material.

Bibliography

[1] Lorenzi Sergio,Additive Manufactoring nella trasmissione di potenza, 2023

[2] https://www.desktopmetal.com/products/shop

[3] https://www.desktopmetal.com/products/Xseries

[4] https://www.eos.info/en/industrial-3d-printer/metal/eos-m-290, 2023

[5] Grande A. Mattia, Additive Manufactoring,2023

[6] Ambrogiani Paolo, Valutazione del comportamento a fatica e analisi di durezza di provini in AlSi10Mg realizzati per additive manufacturing, 2018

[7]https://www.lboro.ac.uk/research/amrg/about/the7categoriesofadditivemanufacturing/powderbedfusion/, 2023

[8] Mohsen Ziaeea, Nathan B. Craneb, Binder jetting A review of process, materials, and methods_notes

[9] Farooq I Azam et al. , An In-Depth Review on Direct Additive Manufacturing of Metals, 2018

[10] Ming Li, Wenchao Du, Metal Binder Jetting Additive Manufactoring A litterature Review, 2020

[11] N. Lecis, R. Beltrami, M. Mariani ,Binder jetting 3D printing of 316 stainless steel: influence of process parameters on microstructural and mechanical properties

[12] R. Pollak, A. Palazzotto, A simulation-based investigation of the staircase method for fatigue strength testing

[13] D. Geldart, *, E. C. Abdullah , A. Hassanpour , L. C. Nwoke and I. Wouter CHARACTERIZATION OF POWDER FLOWABILITY USING MEASUREMENT OF ANGLE OF REPOSEs

[14] Prveen Bidare, Raja Abdullah Powder reusability in Metal Binder Jetting

[15] BERETTA S., Affidabilità delle costruzioni meccaniche, Springer 2008

[16] Dixon, W.J., Mood, A.M., 1948. A method for obtaining and analyzing sensitivity data. J. Am. Stat. Assoc. 43, 109–126.

[17] V. Rouéa,b,⁎, C. Doudarda, S. Callocha, Q. Pujol d'Andrebob, F. Corpaceb, C. Guévenouxb Simulation-based investigation of the reuse of unbroken specimens in a staircase procedure: Accuracy of the determination of fatigue properties,2020

[18] https://www.eos.info/03_system-related-assets/material-related-contents/metal-materials-and-examples/metal-material-datasheet/stainlesssteel/material_datasheet_industryline_17-4ph_m290_en_screen.pdf

[19]https://aidro.it/wp-content/uploads/2022/12/Datasheet_Aidro_MBJ_17-4PH_75um.pdf,,2023

[20] https://aidro.it/wp-content/uploads/2022/12/Datasheet_Aidro_MBJ_316L_40um-1.pdf, 2023

[21] Egseth,Stian&Evensen,Martin Mechanical properties and microstructure of 17-4 PH stainless steel made by Jet binder additive manufacturing, 2022

[22] Eds. H. Bethge and J. Heydenreich , Fractography with the SEM (Failure Analysis) Materials Science. Monographs 40: Electron Microscopy in Solid State Physics.. Elsevier

[23] González-Mancera G. and González-González D. E., Importance of SEM in the Study of Fractography, Camshaft Failure,

[24] Michael Panzenböck ,Scanning Electron Microscope, an Essential Equipment for Failure Analysis, Cambridge University Press, 2018

[25] P H Kaae and E Z Eikeland, Corrosion Performance of Additively Manufactured Stainless Steel by Binder Jetting, *IOP Conf. Ser.: Mater. Sci. Eng.* **1249** 012051 2022

[26] Kamyar Raoufi, Sriram Manoharan, Tom Etheridge, Brian K. Paula, and Karl R. Haapala, Cost and Environmental Impact Assessment of Stainless Steel Microreactor Plates using Binder Jetting and Metal Injection Molding Processes

[27] www.aidro.it

[28] www.dnv.it

[29] R. J. Ferreira; A. M. Grande; J. M. Guedes; A. M. Deus ; G. Sala, Combination of topology and shape optimization with finite element modeling in the case of an aerospace component produced by laser based additive manufacturing,2023

[30] Raffaele Sepe*, Venanzio Giannella, Vittorio Alfieri, Fabrizia Caiazzo, Static and fatigue behavior of laser welded additively manufactured17-4 PH steel plates,2021

[31] Bradley D. Lawrence1 · Todd C. Henry1 · Francis Phillips1 · Jaret Riddick1 · Andelle Kudzal, High-cycle tension-tension fatigue performance of additively manufactured 17–4 PH stainless steel,2023

[32] Jean-marc Linares, Julien Chaves-Jacob, Quentin Lopez and Jean-Michel Sprauel Aix-Marseille Université, CNRS, ISM UMR, Marseille, France, Fatigue life optimization for 17-4Ph steel produced by selective laser melting,2022

[33] A. M. Grande, S. Cacace, A. G. Demir, G. Sala Fracture and fatigue behaviour of AlSi7Mg0.6 produced by Selective Laser Melting: effects of thermal-treatments, 2019

[34] Mohammad Jamalkhani a, Bradley Nathan a, Mike Heim b, Dave Nelson b, Amir Mostafaei a,* Fatigue behavior of vacuum-sintered binder jetted fine 316L stainless steel powder,2023

[35] Christophe Grosjeana, Michel Marzinb, Etienne Camusb, Maxime Roberta, Thomas , Munchc* Static and fatigue behavior of hydraulic components produced by different additive manufacturing processes, 2023

[36] Yunhui Zhua, Ziling Wua, W. Douglas Hartleyb, Jennifer M. Sietinsc, Christopher B. Williamsd, Hang Z. Yub,Unraveling pore evolution in post-processing of binder jetting materials: Xray computed tomography, computer vision, and machine learning, 2020

[37] AMS2759_3J,2020

[38] P H Kaae and E Z Eikeland 2022 *IOP Conf. Ser.: Mater. Sci. Eng.* **1249** 012051 Corrosion Performance of Additively Manufactured
Stainless Steel by Binder Jetting

[39] Luan, He; Grasso, Marco; Colosimo, Bianca M.; Huang, QiangPrescriptive_Modeling_of_Selective_Laser_Melting_Processes_for_Accuracy_Improvement,2019

[40] Jan Platl a , Sabine Bodner a , Christina Hofer a , Andreas Landefelda , Harald Leitner b , Christoph Turk b , Marc-André Nielsenc , Ali Gökhan Demir e , Barbara Previtali e , Jozef Keckes a,d, Ronald Schnitzer Cracking mechanism in a laser powder bed fused cold-work tool steel: The role of residual stresses, microstructure and local elemental concentrations,2022

[41] Jan Platl,* Harald Leitner, Christoph Turk, Ali Gökhan Demir, Barbara Previtali, and Ronald Schnitzer ,Defects in a Laser Powder Bed Fused Tool Steel , 2021

A Appendix A Tensile test

316 L AB							
316L	X	3	14	18	20	21	MEDIA	DEV STD
	Sigma_yld [MPa]	165.18	170.98	169.88	173.82	168.32	169.64	3.20
	E [GPa]	156.88	163.82	168.37	165.64	155.59	162.06	5.58
	Sigma_max [MPa]	537.92	538.07	535.37	539.64	534.85	537.17	2.00
	Elongation [mm/mm]	0.85	0.86	0.84	0.85	0.86	0.85	0.01

316L	Z	11	19	21	27	29	MEDIA	DEV STD
	Sigma_yld [MPa]	170.58	172.37	169.44	169.67	171.65	170.74	1.26
	E [GPa]	170.01	161.72	160.94	159.96	160.55	162.64	4.17
	Sigma_max [MPa]	513.07	533.38	535.99	541.83	533.93	531.64	10.91
	Elongation [mm/mm]	/	0.82	0.83	0.88	0.81	0.83	0.03

HIP								
316L	X	7	9	12	24	28	MEDIA	DEV STD
	Sigma_yld [MPa]	165.77	157.30	158.46	156.97	157.44	159.19	3.72
	E [GPa]	155.30	127.45	123.33	148.71	136.94	138.34	13.61
	sigma_max [MPa]	526.38	524.59	521.38	518.93	524.90	523.24	3.02
	Elongation [mm/mm]	1.02	0.97	0.98	0.98	1.02	0.99	0.02

316L	Z	7.00	9.00	12.00	24.00	28.00	MEDIA	DEV STD
	Sigma_yld [MPa]	162.50	155.64	161.26	164.03	152.46	159.18	4.91
	E [GPa]	131.82	128.37	168.17	118.53	104.38	130.25	23.72
	sigma_max [MPa]	506.80	520.19	513.90	508.62	521.82	514.26	6.71
	Elongation [mm/mm]	0.96	0.97	0.98	0.96	0.96	0.96	0.01

17-4 PH AB

17-4 PH	X	4	27	39	41	56	MEDIA	
	Sigma_yld [MPa]	706.03	703.31	710.01	704.71	702.04	705.22	3.07
	E [GPa]	194.05	191.02	193.18	191.56	191.69	192.30	1.27
	sigma_max [MPa]	967.22	938.88	953.26	945.33	971.45	955.23	13.93
	Elongation [mm/mm]	0.09	0.11	0.10	0.08	0.09	0.09	0.01

17-4 PH	Z	13	16	22	32	59	MEDIA	DEV STD
	Sigma_yld [MPa]	668.46	665.77	667.61	670.73	679.80	670.47	5.51
	E [GPa]	193.67	195.16	194.18	194.78	192.63	194.08	0.99
	sigma_max [MPa]	885.10	896.32	885.95	888.28	897.10	890.55	5.75
	Elongation [mm/mm]	0.07	0.10	0.06	0.10	0.09	0.08	0.02

17-4 PH H900

17-4 PH	X	19	32	37	42	47	MEDIA	DEV STD
	Sigma_yld [MPa]	1075.26	1072.95	1079.10	1066.46	1063.73	1071.50	6.32
	E [GPa]	199.77	200.85	201.61	200.42	200.93	200.72	0.68
	sigma_max [MPa]	1174.61	1180.21	1198.89	1175.67	1161.71	1178.22	13.45
	Elongation [mm/mm]	0.13	0.15	0.14	0.16	0.16	0.15	0.01

17-4 PH	Z	4	14	19	35	51	MEDIA	DEV STD
	Sigma_yld [MPa]	1051.22	1061.95	1039.11	1043.09	1056.49	1050.37	9.38
	E [GPa]	201.69	200.05	203.20	200.06	199.99	201.00	1.42
	sigma_max [MPa]	1231.40	1184.32	1233.54	1227.41	1170.58	1209.45	29.69
	Elongation [mm/mm]	0.10	0.11	0.09	0.14	0.12	0.11	0.02

17-4 PH HIP

17-4 PH	X	2	8	17	31	38	MEDIA	DEV STD
	Sigma_yld [MPa]	733.63	728.94	733.69	731.29	731.49	731.81	1.97
	E [GPa]	195.72	199.00	198.05	196.20	197.47	197.29	1.34
	sigma_max [MPa]	1032.60	1044.44	1009.03	1008.86	1035.96	1026.18	16.31
	Elongation [mm/mm]	0.13	0.14	0.14	0.14	0.14	0.14	0.00

17-4 PH	Z	5	10	29	36	48	MEDIA	DEV STD
	Sigma_yld [MPa]	727.43	700.99	715.36	704.64	712.73	712.23	10.31
	E [GPa]	193.35	195.65	192.74	197.01	198.96	195.54	2.57
	sigma_max [MPa]	947.32	931.9937393	925.4149563	933.7890292	930.6735356	933.84	8.16
	Elongation [mm/mm]	0.134	0.000	0.130	0.129	0.128	0.130	0.058

LPBF 17-4 PH

17-4 PH	X	2	3	4	5	6	MEDIA	DEV STD
LPBF	Sigma_yld [MPa]	815.11	809.23	797.41	809.08	807.46	807.66	5.75
	E [GPa]	194.58	193.33	195.57	193.14	196.75	194.67	1.36
	sigma_max [MPa]	1054.66	1052.33	1039.33	1055.35	1052.89	1050.91	5.90
	Elongation [mm/mm]	0.145	0.153	0.130	0.146	0.139	0.143	0.008

17-4 PH	Z	2	3	4	5	6	MEDIA	DEV STD
LPBF	Sigma_yld [MPa]	810.56	795.88	813.54	821.98	814.59	811.31	8.58
	E [GPa]	194.65	193.50	194.22	199.54	196.94	195.77	2.21
	sigma_max [MPa]	1049.92	1052.03	1047.95	1067.84	1057.34	1055.02	7.13
	Elongation [mm/mm]	0.125	0.132	0.129	0.131	0.138	0.131	0.004

B Appendix B Fatigue test

Part S/N	Material	Load Ratio ; R	Max. Load (N)	Min. Load (N)	Diameter (mm)	Stress Max. (MPa)	%	Cycles to Fail (N_f)	Freq. (Hz)
2	17-4PH H900	0.05	17845	892	6.005	630	60	1000000	25
6	17-4PH H900	0.05	23896	1195	6.018	840	80	112706	20
9	17-4PH H900	0.05	20867	1043	6.012	735	70	119868	20
12	17-4PH H900	0.05	27017	1351	6.033	945	90	14911	20
15	17-4PH H900	0.05	21018	1051	6.034	735	70	154046	20
21	17-4PH H900	0.05	24055	1203	6.038	840	80	31752	20
24	17-4PH H900	0.05	26779	1339	6.007	945	90	36502	20
26	17-4PH H900	0.05	18039	902	5.590	735	70	185642	20
28	17-4PH H900	0.05	24169	1208	6.053	840	80	39236	20
33	17-4PH H900	0.05	27196	1360	6.053	945	90	30046	20
37	17-4PH H900	0.05	25685	1284	6.053	893	85	28900	20
38	17-4PH H900	0.05	22564	1128	6.040	788	75	118976	20
40	17-4PH H900	0.05	19510	976	6.033	683	65	391745	20
42	17-4PH H900	0.05	25319	1266	6.010	893	85	55702	20
44	17-4PH H900	0.05	22566	1128	6.040	788	75	51822	20
49	17-4PH H900	0.05	19521	976	6.035	683	65	138532	20
53	17-4PH H900	0.05	18649	932	6.044	650	61.90	1000000	20
55	17-4PH H900	0.05	18916	946	5.996	670	63.8	531100	20
58	17-4PH H900	0.05	18665	933	6.047	650	61.9	283846	20
60	17-4PH H900	0.05	17767	888	5.992	630	60.0	481241	20

C Appendix C Porosity measures

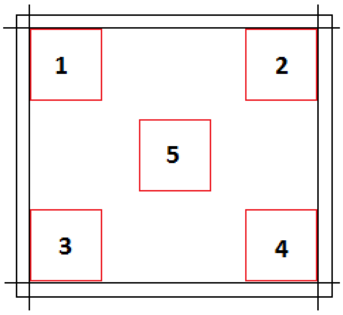

POROSITY MEASUREMENT [%]	1	2	3	4	5	**MEAN**	**STD**
316L AB MBJ	99.86	99.931	99.913	99.635	99.915	99.851	0.123
316L HIP MBJ	99.923	99.98	99.94	99.931	99.994	99.954	0.031
17-4PH AB MBJ	99.978	99.81	99.9	99.941	99.987	99.923	0.072
17-4 PH H900 MBJ	99.801	99.990	99.864	99.953	99.88	99.898	0.074
17-4 PH HIP MBJ	99.961	99.965	99.943	99.977	99.997	99.969	0.020
17-4 PH PBLF	99.97	99.998	99.993	99.994	99.99	99.991	0.012

17-4 PH As built	
Position 1	**Position2**
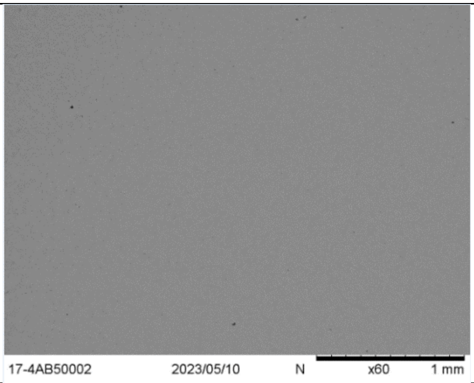 17-4AB50002 2023/05/10 N x60 1 mm	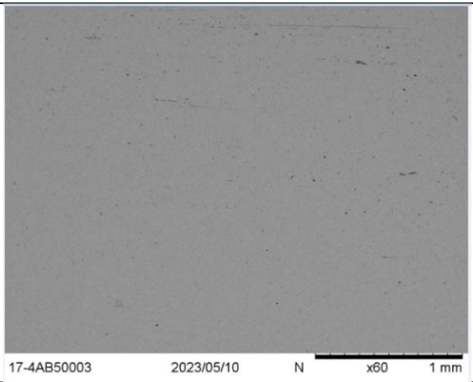 17-4AB50003 2023/05/10 N x60 1 mm
Position 3	**Position4**
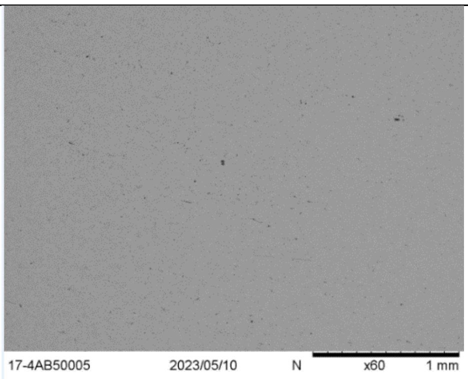 17-4AB50005 2023/05/10 N x60 1 mm	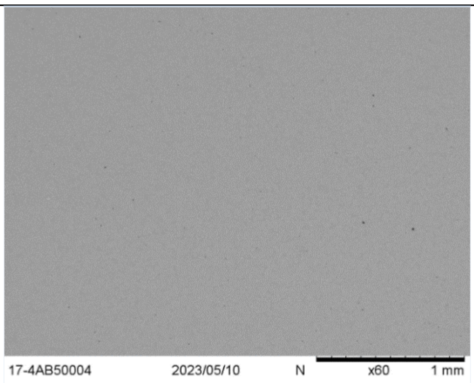 17-4AB50004 2023/05/10 N x60 1 mm
Position 5	
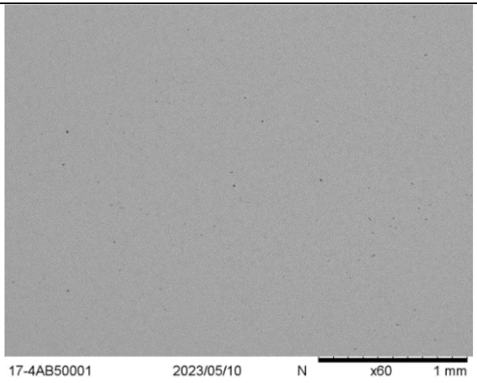 17-4AB50001 2023/05/10 N x60 1 mm	

17-4 PH H900	
Position 1	**Position2**
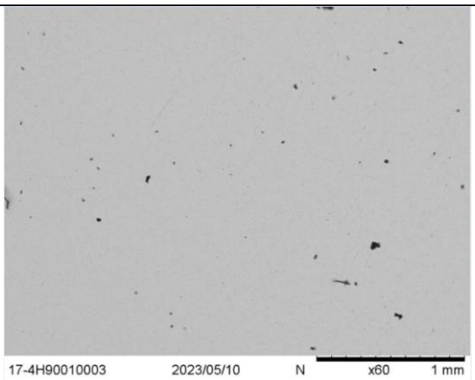 17-4H90010003 2023/05/10 N x60 1 mm	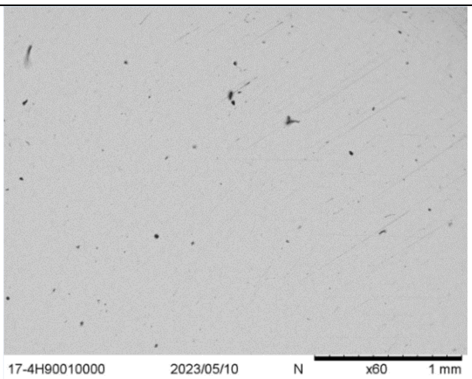 17-4H90010000 2023/05/10 N x60 1 mm
Position 3	**Position4**
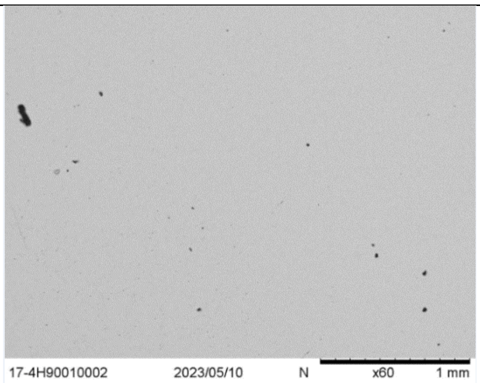 17-4H90010002 2023/05/10 N x60 1 mm	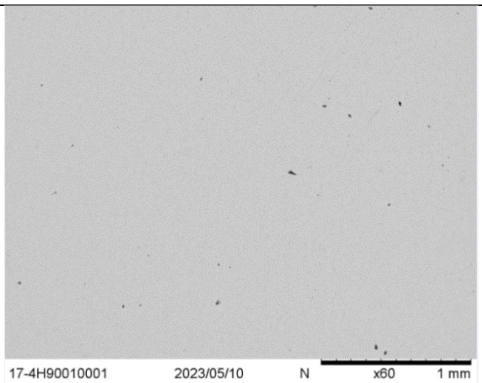 17-4H90010001 2023/05/10 N x60 1 mm
Position 5	
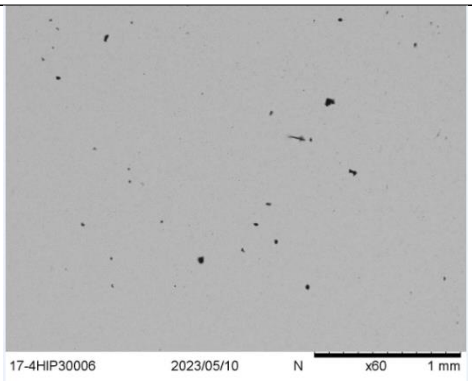 17-4HIP30006 2023/05/10 N x60 1 mm	

17-4 PH HIP	
Position 1	**Position2**
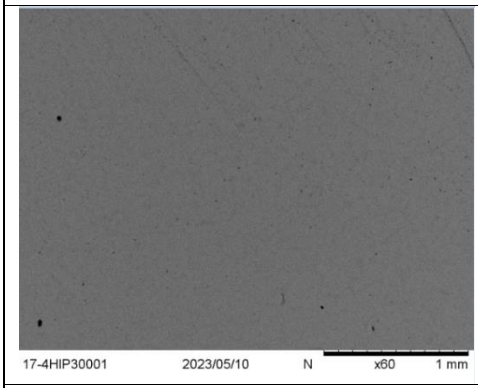 17-4HIP30001 2023/05/10 N x60 1 mm	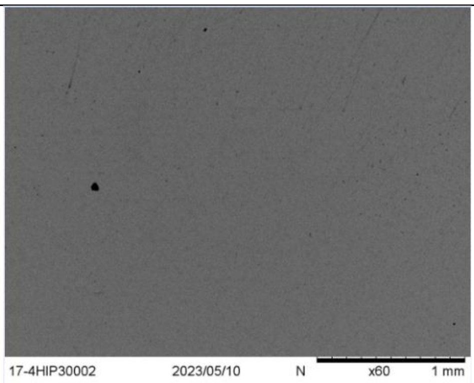 17-4HIP30002 2023/05/10 N x60 1 mm
Position 3	**Position4**
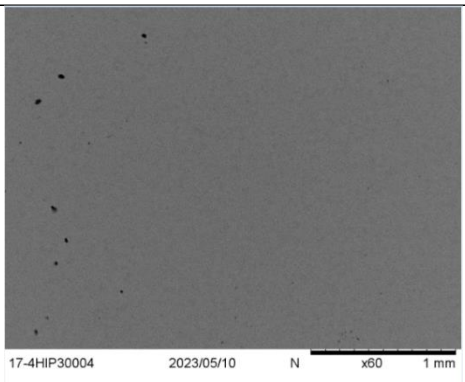 17-4HIP30004 2023/05/10 N x60 1 mm	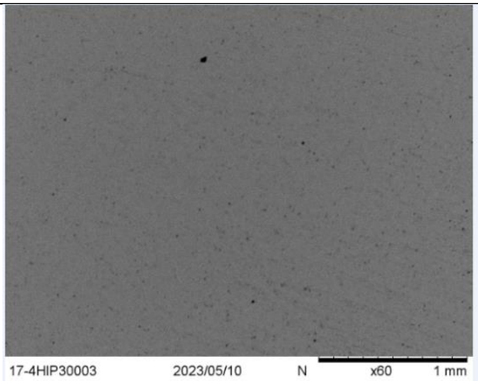 17-4HIP30003 2023/05/10 N x60 1 mm
Position 5	
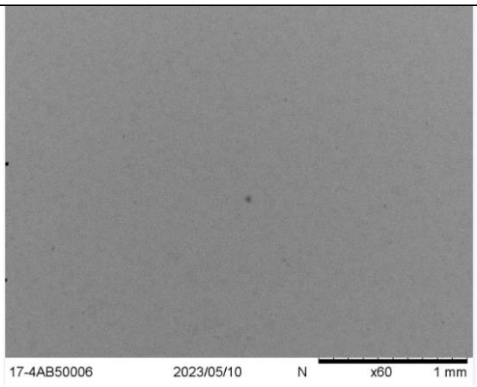 17-4AB50006 2023/05/10 N x60 1 mm	

316L As built	
Position 1	**Position2**
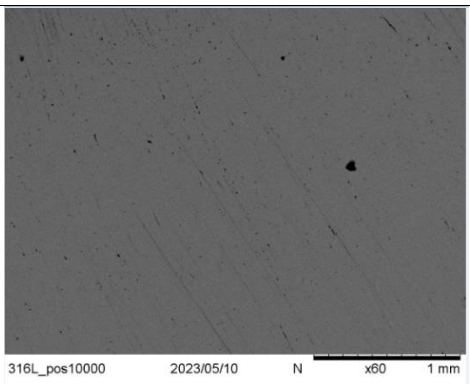 316L_pos10000 2023/05/10 N x60 1 mm	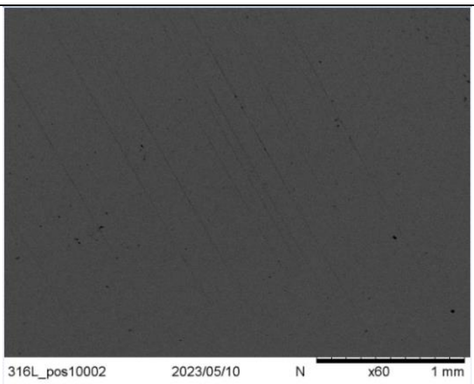 316L_pos10002 2023/05/10 N x60 1 mm
Position 3	**Position4**
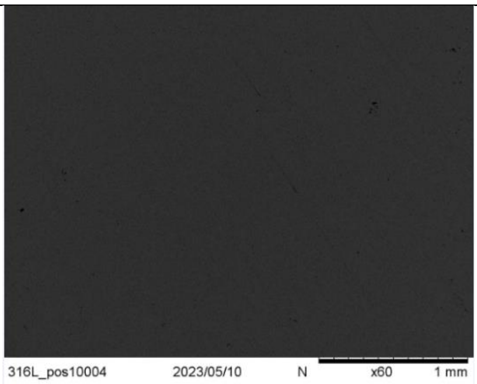 316L_pos10004 2023/05/10 N x60 1 mm	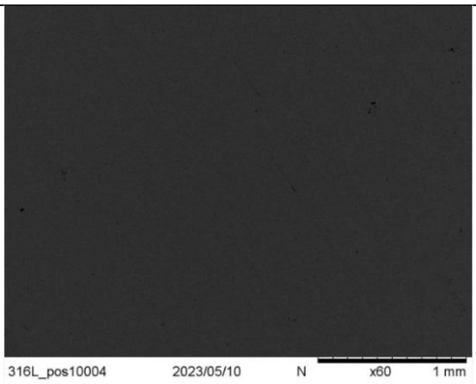 316L_pos10004 2023/05/10 N x60 1 mm
Position 5	
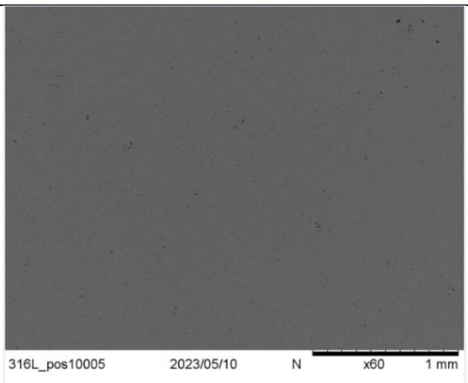 316L_pos10005 2023/05/10 N x60 1 mm	

<table>
<tr><th colspan="2">316L HIP</th></tr>
<tr><td>Position 1</td><td>Position2</td></tr>
<tr><td>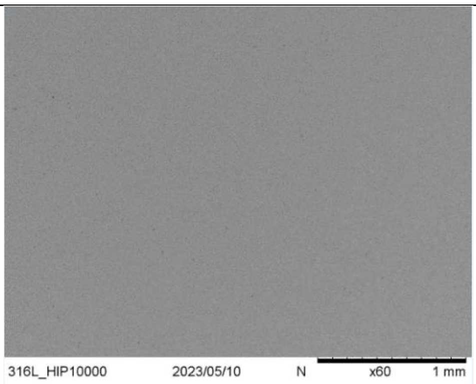
316L_HIP10000
2023/05/10
N
x60
1 mm

</td><td>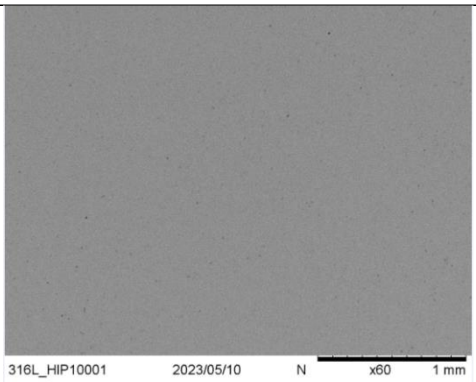
316L_HIP10001
2023/05/10
N
x60
1 mm

</td></tr>
<tr><td>Position 3</td><td>Position4</td></tr>
<tr><td>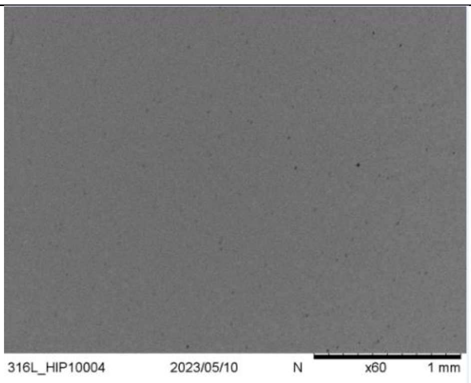
316L_HIP10004
2023/05/10
N
x60
1 mm

</td><td>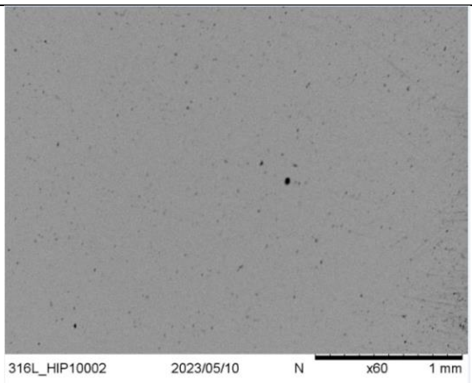
316L_HIP10002
2023/05/10
N
x60
1 mm

</td></tr>
<tr><td>Position 5</td><td></td></tr>
<tr><td>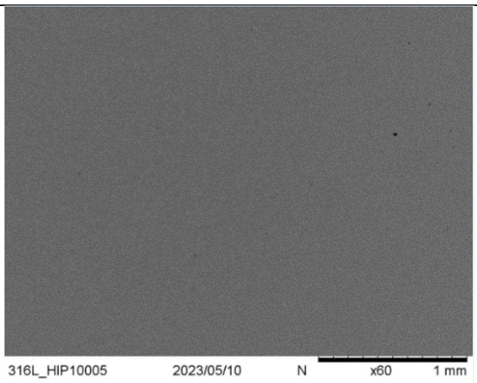
316L_HIP10005
2023/05/10
N
x60
1 mm

</td><td></td></tr>
</table>

D Appendix D density measures

Provino	rho	MEDIA	DEV STD
LPBF 17-4 PH AB	7.782	7.744	0.077
	7.794		
	7.656		
MBJ 17-4 PH AB	7.681	7.690	0.021
	7.674		
	7.714		
MBJ 17-4 PH H900	7.689	7.706	0.016
	7.719		
	7.711		
MBJ 17-4 PH HIP	7.763	7.765	0.004
	7.762		
	7.769		
MBJ 316 L AB	7.885	7.882	0.028
	7.853		
	7.908		
MBJ 316 L HIP	7.968	7.952	0.014

Ringraziamenti

Non è facile ringraziare in poche righe tutte le persone che mi hanno permesso di portare a compimento questo mio importante percorso.

Innanzi tutto, vorrei ringraziare **Aidro** che mi ha aiutato in queste mie prime esperienze lavorative, dandomi la possibilità di affrontare nuove sfide e arricchire le mie capacità.

Ci tengo a ringraziare Tommaso e Valeria Tirelli che mi hanno accolto in un ambiente professionale e sono sempre stati attenti al benessere del personale.

Un sincero grazie anche agli ingegneri Gabriele, Fabio, Paolo, Luca e Giacomo che mi hanno dato molti nuovi spunti su cui riflettere ed affinare le mie conoscenze in merito alla stampa 3D e alle lavorazioni meccaniche.

Non posso non citare Miguel e Collins che mi hanno aiutato a smaltire il lavoro da fare con le macchine CNC oltre a sapere davvero tanti metodi per ottimizzare la riuscita dei pezzi da lavorare.

Grazie anche a Simona, Rosy, Oxana, e Gaia che mi hanno dato una mano nelle varie spedizioni e arrivi dei pezzi necessari ai miei studi.

Ringrazio sinceramente il professor **Grande** che nonostante i suoi impegni è riuscito a dedicarmi il tempo necessario e si è sempre mostrato sempre disponibile e paziente.

Ringrazio tutto il personale del laboratorio, in particolate **Rosy e Paolo** che, malgrado alcuni indicenti di percorso, mi hanno insegato le procedure necessarie per lavorare in sicurezza in questi ambienti accademici.

Ringrazio tutte le aziende con cui ho collaborato in questi mesi di tesi che mi hanno fornito tutto il materiale di cui avevo bisogno per i miei studi. In particolare Eric Mangot di **Bodycote** che mi ha fornito trattamenti termici.

Grazie a Giorgio Valsecchi e Marco Baretti di **Tav** che in tempi rapidi ha avuto piacere di farmi un paio di trattamenti termici rendendosi disponibile a domande ed approfondimenti.

Ringrazio anche Cecile Laverriere di **Eos** che gratuitamente ci ha spedito i suoi provini da analizzare per le prove statiche e a fatica.

Ringrazio con tutto il cuore i miei amici che mi hanno sostenuto e accompagnato lungo il mio percorso di studi, con cui ho condiviso gioie e dolori. C'è chi è stato più presente di altri, amicizie che si sono allontanate per poi ristringersi ma con ognuno di loro ho condiviso una parte di me. Sono sicuro che non hanno bisogno del loro nome scritto per sapere quanto sono stati importanti e determinanti per la conclusione di questo viaggio.

Infine, un ringraziamento davvero speciale alla mia famiglia, che mi ha permesso di seguire la mia passione e mi ha supportato nelle giornate nere.

Grazie mamma e papà, che avete creduto in me e senza di voi non sarei mai arrivato dove sono ora. Grazie per la pazienza che avete portato, grazie per l'aiuto incondizionato che mi avete dato e che mi state dando.

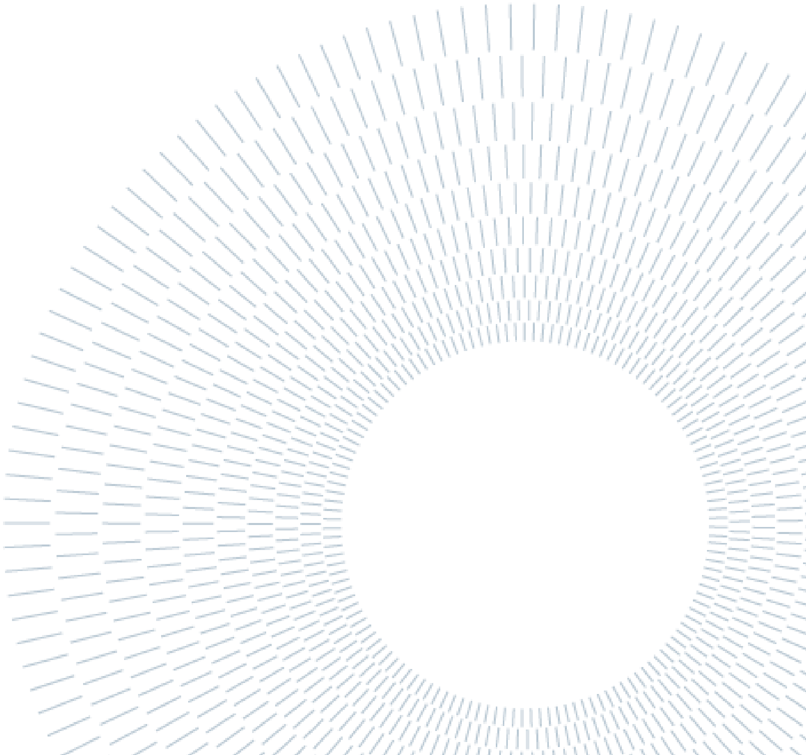Grazie a tutte le persone che ho incontrato in questo percorso perché mi hanno permesso di essere la persona che sono ora, donandomi chi esperienza chi emozioni, chi conoscenza.